Chemical Engineering Report Series
Kemian laitetekniikan raporttisarja No. 55
Espoo 2010

MODELING CHLORINE DIOXIDE BLEACHING OF CHEMICAL PULP

Ville Tarvo

Aalto University
School of Science
and Technology

Chemical Engineering Report Series
Kemian laitetekniikan raporttisarja No. 55
Espoo 2010

MODELING CHLORINE DIOXIDE BLEACHING OF CHEMICAL PULP

Ville Tarvo

Doctoral dissertation for the degree of Doctor of Science in Technology to be presented with due permission of the Faculty of Chemistry and Materials Sciences for public examination and debate in Auditorium KE2 (Komppa Auditorium) at the Aalto University School of Science and Technology (Espoo, Finland) on the 17th of June 2010 at 12 noon.

Aalto University
School of Science and Technology
Faculty of Chemistry and Material Sciences
Department of Biotechnology and Chemical Technology

Aalto-yliopisto
Teknillinen korkeakoulu
Kemian ja materiaalitieteiden tiedekunta
Biotekniikan ja kemian tekniikan laitos

Distribution:
Aalto University
School of Science and Technology
Chemical Engineering
P. O. Box 16100
FI-00076 AALTO
Tel. + 358-9-4702 2634
Fax. +358-9-4702 2694
E-mail: ville.tarvo@tkk.fi

ISBN 978-952-60-3191-0
ISSN 1236-875X

Multiprint Oy
Espoo 2010

ABSTRACT

This doctoral thesis deals with the phenomenon-based modeling of pulp bleaching. Previous bleaching models typically utilize one or two empirical correlations to predict the kinetics in kappa number development. Empirical correlations are simple to develop, but their parameters are often tied to the validation system. A major benefit of physico-chemical phenomenon models is that they are valid regardless of the reaction environment. Furthermore, modeling the bleaching processes at molecular level provides a new way to examine the relative importance of various phenomena, the validity of theories and the bottlenecks of bleaching applications.

The first part of the thesis introduces a model for the pulp suspension environment and describes the physico-chemical models in use (reaction kinetics, mass transfer, thermodynamics). The second part deals with inorganic oxychlorine reactions related to chlorine dioxide bleaching. The reaction kinetics and mechanism are documented for iron- mediated chlorite decomposition, chlorous acid self-decomposition, and for the reaction between hypochlorous acid and chlorous acid. The rate coefficient temperature dependency is reported for the two latter reactions. The reaction kinetic models were utilized in assessing the potential chlorate formation routes encountered in pulp bleaching. It was concluded that chlorous acid self-decomposition is unlikely to contribute to chlorate formation in bleaching applications. The iron-mediated chlorite decomposition and the reaction between hypochlorous acid and chlorous acid are expected to produce chlorate.

The last part introduces a model for chlorine dioxide delignification. Here the pulp suspension model was combined with a broad set of chemical reactions describing the ClO_2 bleaching chemistry. The incorporated reactions cover lignin oxidation, lignin chlorination, hexenuronic acid degradation, lignin dissolution, oxidation of extractives and the essential inorganic oxychlorine reactions. The model predictions were compared against experimental delignification results in order to validate the model and obtain the previously unknown reaction rate parameters. The predictions were generally in good agreement with experimental results. Deviations related primarily to hypochlorous acid driven processes: organochlorine formation, hexenuronic acid degrading reactions, chlorite depletion or chlorate formation. The simulation results suggest that organochlorine formation is restricted by the amount of chlorination-susceptible substrates in pulp rather than the availability of chlorine. It was also concluded that, in addition to the fully inorganic reactions, chlorite is also likely to be consumed in reactions with pulp-related compounds, for instance with aldehydes.

TIIVISTELMÄ

Väitöskirjassa tutkittiin sellun klooridioksidivalkaisun ilmiöpohjaista mallittamista. Olemassa olevat valkaisuprosessien mallit perustuvat empiirisiin korrelaatioihin, jotka ovat puhtaasti matemaattisia ja joiden käyttömahdollisuudet ovat usein rajallisia. Tässä työssä valkaisun kuvaamiseen käytettiin fysikaalis-kemiallisia ilmiömalleja (reaktiokinetiikka, aineensiirto, termodynamiikka), joilla on periaatteessa rajoittamattomat soveltuvuusalueet. Prosessien tutkiminen molekyylitasolla tarjoaa uudenlaiset edellytykset arvioida ilmiöiden keskinäisiä vaikutuksia, valkaisukemiaan liittyviä teorioiden paikkansapitävyyttä sekä käytännön sovellusten rajoittavia tekijöitä.

Työn ensimmäisessä osassa luotiin malli sellususpensioympäristölle sekä määritettiin mallitusperiaatteet valkaisuprosessien tärkeimmille fysikaalis-kemiallisille ilmiöille. Toisessa osassa tutkittiin klooridioksidivalkaisussa esiintyvien epäorgaanisten klooriyhdisteiden tärkeimpien reaktioiden mekanismeja ja kinetiikkaa vesiliuoksessa. Kloriitin rautakatalysoidulle hajoamiselle, kloorihapokkeen spontaanille hajoamiselle sekä alikloorihapokkeen ja kloorihapokkeen väliselle reaktiolle määritettiin reaktionopeusvakiot. Kahdelle viimeiselle reaktiolle määritettiin myös reaktionopeusvakioiden lämpötilariippuvuus (aktivoitumisenergia). Reaktiokineettisten mallien avulla arvioitiin valkaisun aikana syntyvän kloraatin muodostumisreittejä. Simulaatiotulosten perusteella todettiin, että kloorihapokkeen spontaani hajoamisreaktio on valkaisuolosuhteissa niin hidas, ettei sen osallistuminen kloraatin muodostukseen ole todennäköistä. Sen sijaan kloriitin rautakatalysoitu hajoaminen sekä alikloorihapokkeen ja kloorihapokkeen välinen reaktio ovat potentiaalisia kloraatinmuodostumisreittejä.

Työn viimeisessä osassa luotiin kokonaismalli ligniiniä poistavalle klooridioksidivalkaisulle. Mallikokonaisuudessa yhdistettiin sellususpensiomalli sekä joukko kemiallisia reaktioita, joilla kuvattiin kloorikomponenttien reaktiot jäännösligniinin, heksenuronihapon ja uuteaineiden kanssa sekä epäorgaanisten klooriyhdisteiden keskinäiset reaktiot. Mallin ennusteita verrattiin valkaisukokeissa saatuihin tuloksiin. Vastaavuuden todettiin olevan pääsääntöisesti hyvä. Heikkoudet liittyivät ensisijaisesti alikloorihapokkeen ja kloorin reaktioihin: orgaanisten klooriyhdisteiden muodostumiseen, heksenuronihappojen reaktioihin sekä kloriitin kulutukseen tai kloraatin muodostumiseen. Tulosten perusteella pääteltiin, että orgaanisten klooriyhdisteiden muodostumista rajoittava tekijä liittyy todennäköisemmin kuiduissa olevien substraattien määrään kuin välituotteena syntyvän kloorin määrään. Simulointitulokset viittasivat myös siihen, että valkaisun aikana tapahtuva kloriitin hajoaminen on ainakin osittain seurausta reaktioista ligniini- tai hiilihydraattiperäisten komponenttien, mahdollisesti aldehydien, kanssa.

PREFACE

This thesis work was carried out at Aalto University School of Science and Technology (TKK) in the research group of Chemical Engineering during 2004-2009.

I wish to thank Professors Juhani Aittamaa, Ville Alopaeus, and Tapani Vuorinen for providing me the opportunity to work with a topic that has been rich in scientific ambition as well as in practical relevance. Your encouragement and professional guidance has been irreplaceable.

I express deep gratitude for my colleagues Susanna Kuitunen and Tuula Lehtimaa. Our collaboration has been exceptional in so many ways. Co-authors Kyösti Ruuttunen, Gerard Mortha, Erkki Räsänen, Pekka Tervola, Tarja Tamminen, Tapani Vuorinen, and Kaj Henricson are acknowledged for their expertise and contributions. I want to thank the research group staff for keeping up a great atmosphere. Representatives of the industrial partners of ABLE and VIP projects are thanked for bringing up the practical aspects.

The financial support from the Graduate School in Chemical Engineering, the National Technology Agency of Finland (TEKES), and from the industrial partners of ABLE and VIP projects is acknowledged with gratitude.

A special thanks to my family and friends. Although not directly involved in the scientific work, this thesis could not have been accomplished without you.

Finally, a loving thanks to Teija.

Espoo 23.04.2010

Ville Tarvo

LIST OF PUBLICATIONS

This thesis is based on the following publications (Appendices I-V), which are referred to in the text by their roman numerals.

[I] Tarvo, Ville; Kuitunen, Susanna; Lehtimaa, Tuula; Tervola, Pekka; Rasanen, Erkki; Tamminen, Tarja; Aittamaa, Juhani; Vuorinen, Tapani; Henricson, Kaj, Modelling of chemical pulp bleaching, *Nord. Pulp Paper Res. J.* **23**(1) (2008) 91-101.

[II] Lehtimaa, Tuula; Tarvo, Ville; Mortha, Gerard; Kuitunen, Susanna; Vuorinen, Tapani, Reactions and kinetics of Cl(III) decomposition, *Ind. Eng. Chem. Res.* **47**(15) (2008) 5284-5290.

[III] Tarvo, Ville; Lehtimaa, Tuula; Kuitunen, Susanna; Alopaeus, Ville; Vuorinen, Tapani, Chlorate formation in chlorine dioxide delignification – an analysis via elementary kinetic modelling, *J. Wood Chem. Technol.* **29**(3) (2009) 191-213.

[IV] Tarvo, Ville; Lehtimaa, Tuula; Kuitunen, Susanna; Alopaeus, Ville; Vuorinen, Tapani; Aittamaa, Juhani, The kinetics and stoichiometry of the reaction between hypochlorous acid and chlorous acid in mildly acidic solutions, *Ind. Eng. Chem. Res.* **48**(13) (2009) 6280-6286.

[V] Tarvo, Ville; Lehtimaa, Tuula; Kuitunen, Susanna; Alopaeus, Ville; Vuorinen, Tapani; Aittamaa, Juhani, A model for chlorine dioxide delignification of chemical pulp, Accepted for publication in *J. Wood Chem. Technol.*

AUTHOR CONTRIBUTION

[I] The author designed the models and programmed the computer code with co-authors, performed the simulations and wrote the paper.

[II] The author participated in planning the experiments, conducted the parameter regression procedures, participated in analyzing the results and wrote parts of the paper.

[III] The author conducted the simulations, analyzed the results and wrote the paper.

[IV] The author participated in planning the experiments, conducted the parameter regression procedures, and analyzed the results and wrote the paper together with co-authors.

[V] The author constructed the model together with co-authors, conducted the simulations, analyzed the results and wrote the paper.

TABLE OF CONTENTS

1 BACKGROUND

Kraft pulping disintegrates wood fibers by removing and modifying lignin, the polymeric substance keeping the fibers attached. The majority of the lignin is removed during pulping, but a small, highly colored residue (typically 1.5-6% of o.d. pulp) is left in the brownstock pulp (Sixta et al. 2006). There are also other colored impurities as well as foreign matter that contribute to the observed color, but residual lignin is the major source of color. Chemical pulp bleaching aims at removing the residual lignin (delignifying bleaching) or destroying the colored structures in lignin and in other pulp components (Sixta et al. 2006; Fogelholm 2000).

Chlorine dioxide (ClO_2) is the primary bleaching agent applied in modern chemical pulp bleaching processes. Elemental Chlorine-Free (ECF) pulp, produced using chlorine dioxide as the primary bleaching agent, had a nearly 85% world market share in 2005 (Anon. 2006). This number is likely to have increased during the past five years. The popularity of chlorine dioxide is explained by its high selectivity and low environmental impact (Sixta et al. 2006). Moreover, ECF bleaching is acknowledged as a core component of Best Available Technology (Anon. 2006). Chlorine dioxide has therefore high importance in practical pulp bleaching both today and in the near future. Despite its wide use and the large amount of related research, many aspects regarding chlorine dioxide bleaching chemistry are poorly understood. A significant part of ClO_2 ends up as inactive chlorate (ClO_3^-), especially in the final bleaching stages (Marpillero 1958; Fredricks et al. 1971; Rapson and Anderson 1977; Kolar et al. 1983; Medina et al. 2008). Also, the ClO_2 quantities consumed in chlorine dioxide delignification are much higher than what is theoretically needed to solubilize lignin (Lachenal and Chirat 2000). Overcoming the practical problems encountered in using chlorine dioxide as pulp bleaching agent requires profound understanding of the chemistry and of the physico-chemical processes that define the bleaching outcome. One way to obtain such knowledge is to use modeling and simulation tools. The presently available chlorine dioxide bleaching models typically employ one or two empirical correlations to predict the kinetics in kappa number development (Germgård 1982; Barroca et al. 2001; Chandranupap and Nguyen 2000; Savoie and Tessier 1997; Tessier and Savoie 1997; Mortha et al. 2001). The correlations are fast and easy to use, and they are beneficial in forming a gross linkage between the key process variables and the bleaching result. As a downside, the correlation parameters rarely have physical meaning and hence the parameter values are often tied to the experimental setup (pulp type, conditions, apparatus, etc). Another limitation of the kappa correlations is that the maximum delignification result (highest attainable kappa number drop) is required as an input parameter. In many cases the research objective would be to find ways to exceed the apparent maximum performance.

Chemical reaction systems may be modeled at various scales of physico-chemical precision. At one end lie empirical correlations, which exploit a purely mathematical approach. Atomic level models that consider chemical reactions through orbital theories may be thought to lie at the opposite end. Both approaches, as well as anything in between, serve their purposes. The task at hand defines the suitable level of precision. Although the research related to pulp bleaching has mainly employed the correlation approach (kappa number models), chemical and petrochemical industries often make use of phenomenon-based models that rely on thermodynamics, chemical reactions, mass transfer, fluid dynamics, etc. The benefit of phenomenon-based modeling is that the models and parameters are considered independent of size or shape of experimental equipment, or of any other external constraints. Thus, extrapolation in composition, scale, geometry, or in process conditions is fairly reliable. Freedom of system composition is a particularly beneficial property. In pulp bleaching applications this means that the model parameters are independent of the pulp type (wood species), the pulping process, or the filtrates in use – so long as the pulps and filtrates are characterized to a sufficient extent. Phenomenon-based modeling also facilitates straightforward investigation of reaction mechanisms as chemical reactions are modeled on molecular scale. The essential requirements for using a phenomenon-based modeling approach is that appropriate models are available, suitable parameters are available or they can be determined, and the physical environment in which the phenomenon models operate is defined. The purpose of this work has been to provide new research tools by developing a phenomenon-based modeling environment for chemical pulp bleaching processes and to implement a reaction library sufficient for modeling chlorine dioxide bleaching.

2 PULP SUSPENSION MODEL

The principles and concepts related to modeling the pulp suspension environment and the physico-chemical phenomena of pulp bleaching are introduced in paper [I]. The main constituents in pulp suspensions are wood fibers, water, and chemicals dissolved in water. The fibers are modeled as hollow cylinders. When suspended into an aqueous medium, the fiber wall will absorb liquid. The stagnant liquid inside the fiber wall is considered separate from the bulk liquid and is referred to as the fiber-bound liquid. The bulk liquid, both outside the cylindrical fibers and inside the fiber lumen, is referred to as the external liquid. The lumen liquid is assumed to be in open contact with the liquid outside the fibers through pits in the fiber wall. The volume of the fiber-bound liquid is defined via the fiber saturation point (FSP). The solid fiber wall components are modeled as an insoluble phase where the fiber polymers and other components are uniformly distributed. The fiber-bound liquid is believed to occupy the micronic network of pores in the cell wall, providing an unrestricted interaction with the fiber wall components. Therefore, the solid fiber wall and the fiber-bound liquid have an interface, as do the two liquid phases, but there is no direct contact between the external liquid and the solid fiber wall. A schematic depiction of the suspension environment is given in Figure 1.

Lignin is modeled with monomeric pseudo-compounds. This simplification enables efficient incorporation of the chemical characteristics and reactions of various lignin structures, although ensuing compromises in the modeling the macromolecular features of the lignin. Syringyl and guaiacyl lignin units are distinguished with regard to molar weight; their reaction paths and kinetics are assumed to be equal. Chlorine dioxide is known to be a very selective lignin oxidant, reacting much faster with lignin than with pulp carbohydrates (Alén 2000). Consequently, cellulose and hemicelluloses are assumed to be mainly inert. Uronic acids, attached to xylan, make an exception. Methylglucuronic acid and hexenuronic acid contribute to the acid-base properties of pulp and the participation of hexenuronic acid in chemical consumption (Vuorinen et al. 1997) is included.

The acidic groups in wood fibers contribute to the electrostatic equilibrium in the fiber-bound liquid and cause an uneven distribution of mobile ions between the two liquid phases. The Donnan theory is used to define the uneven distribution (Helfferich 1962; Towers and Scallan 1996; Bygrave and Englezos 2000; Lindgren et al. 2001; Räsänen et al. 2001). The following categories of fiber acids are incorporated into the model: uronic acids in hemicelluloses (pK_a = 3.1) (Laine et al. 1994), residual lignin- and extractive-derived carboxylic acids (pK_{a1} = 4-6, pK_{a2} = 2-3) (Laine et al. 1994; Räsänen 2003), and lignin-derived phenols (pK_a = 9-11) (Ragnar et al. 2000; Norgren and Lindström 2000a).

The protolysis reactions are assumed to reach an instantaneous equilibrium, i.e. their kinetic nature is disregarded.

Reaction kinetics is used to model the progress of pulp bleaching at molecular level. The reactions cover lignin oxidation, lignin dissolution, hexenuronic acid oxidation, oxidation of unsaturated extractives, and inorganic oxychlorine reactions. The complete set of reactions used to model chlorine dioxide delignification is introduced later. The temperature dependency of the reaction rate coefficients is modeled with the Arrhenius equation.

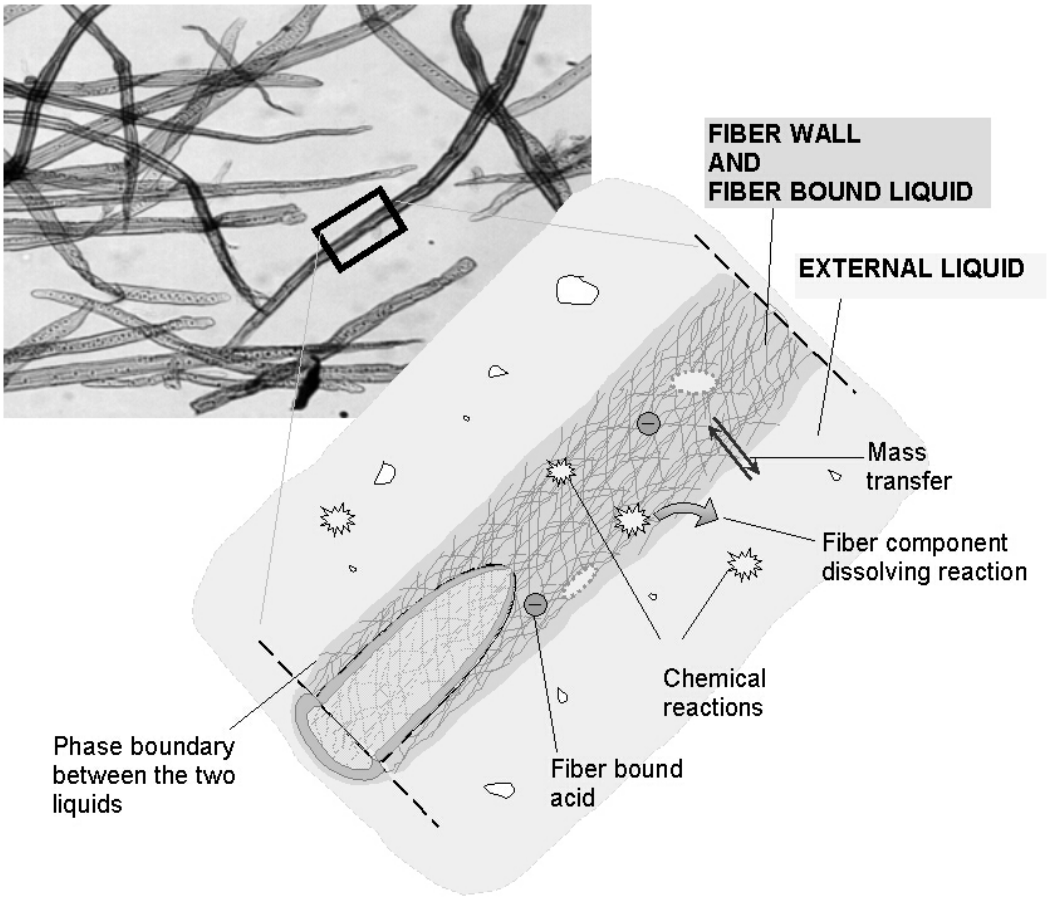

Figure 1. A schematic picture of the phenomenon-based delignification model principles.

The film theory is used to describe the mass transfer between the fiber-bound liquid and the external liquid. Mass transfer resistance is assumed to lie in a stagnant fluid film between the phases. The bulk liquids far from the phase boundary are assumed to be ideally mixed. The majority of the aqueous phase in pulp suspensions is composed of water (molar fraction of water is typically > 0.99). Thus, convective effects other than those related to fiber swelling are assumed to have a negligible contribution to the liquid-liquid mass transfer. Due to the dilute system, the component interactions of diffusing *neutral* components are also neglected. The electrostatic interactions of diffusing *ions*

cannot be omitted even in a dilute system. A simplified representation of the Nernst-Planck equation is used to describe the mass transfer of ionic species (e1) (Ala-Kaila 1998).

$$N_i = \frac{-D_{i,eff}}{x}\left(\Delta a_i + \overline{a}_i z_i \left(\sum_{j=1}^{n} \frac{z_j D_{j,eff} \Delta a_j}{\overline{a}_j z_j^2 D_{j,eff}}\right)\right) \qquad \text{(e1)}$$

The effective diffusion coefficient values (D_{eff}) used for pore diffusion are obtained from pure liquid phase diffusion coefficients (D) by multiplying by fiber porosity (ε) and dividing by pore tortuosity (τ) (e2) (Froment and Bischoff 1990). Fiber porosity (ε) is estimated with equation (e3). The fiber pore tortuosity is assumed to have a value τ = 7.0 according to Zhang et al. (1998).

$$D_{eff} = \frac{\varepsilon}{\tau} D \qquad \text{(e2)}$$

$$\varepsilon = \frac{V_B}{V_B + V_F} \qquad \text{(e3)}$$

Reported diffusion coefficients are used for all compounds (molecules and ions), when available. These are found in several textbooks (Perry and Green 1997; Newman 1991; Cussler 1984). The Wilke-Chang correlation is used to estimate the diffusion coefficients when no reported value is available (Reid et al. 1987). The literature and phenomena related to lignin diffusion coefficients is discussed in paper [I]. D = 10^{-10} m^2/s is used for the dissolved lignin diffusion coefficient (Norgren and Lindström 2000b). The effect of temperature on the diffusion coefficients is estimated with equation (e4) (Reid et al. 1987). Pure water viscosity is used as solvent viscosity (μ and μ^{ref}) in (e4). The viscosity values are computed from the correlation of Laliberte (2007a; 2007b).

$$D = \frac{T / T^{ref}}{\mu / \mu^{ref}} D^{ref} \qquad \text{(e4)}$$

3 INORGANIC OXYCHLORINE REACTIONS IN CHLORINE DIOXIDE BLEACHING

When chlorine dioxide is used in pulp bleaching, the majority is reduced to chloride (Cl^-). During the course of this reaction, the chlorine atoms are reduced from +4 valence to –1. The reduction occurs in a stepwise manner and involves several inorganic oxychlorine species. The chlorite ion (ClO_2^-) and hypochlorous acid (HOCl) are the primary reduction products of chlorine dioxide in ClO_2 (Lindgren 1971; Dence and Reeve 1996; Ni et al. 1994; Kolar et al. 1983; Brage et al. 1991a). Both compounds react further through several competing reactions, which may be fully inorganic or involve pulp components. The complex reaction network produces reactive intermediates, such as chlorine and chlorine dioxide, as well as more stable forms of chlorine, like chlorate (ClO_3^-) and organically-bound chlorine (Kolar et al. 1983). While chlorine dioxide regeneration is highly desirable, the formation of chlorate and organochlorine compounds is unwelcome. The importance of understanding the reaction mechanisms and factors influencing the final product distribution is self-evident.

$$2\ HClO_2 \rightarrow HOCl + ClO_3^- + H^+ \quad (1)$$

$$HClO_2 + Cl^- + H^+ \rightarrow 2\ HOCl \quad (2)$$

$$ClO_2^- + Fe^{2+/3+} \rightarrow \text{various products} \quad (3)$$

$$HClO_2 + HOCl \rightarrow Cl_2O_2 + H2O \rightarrow\rightarrow \text{various products} \quad (4)$$

The main inorganic reactions believed to consume the chlorite and hypochlorous acid are (1) chlorous acid ($HClO_2$) self-decomposition, (2) the reaction between chlorous acid and chloride ion in an acidic medium, (3) iron-mediated chlorite decomposition, and (4) the reaction between chlorous acid and hypochlorous acid. A vast amount of literature deals with the kinetics and stoichiometry of these reactions, yet the reported results and conclusions are quite diverse. This topic is discussed in detail in papers [II-IV]. Due to the incoherence in the available literature, new experiments were carried out. Without purposeful control, reactions paths (1-4) operate simultaneously resulting in a complex network of reactions with several parallel and successive steps. The previous studies have typically examined the full reaction system, making the mechanistic and kinetic analysis difficult. In our experiments, the reaction entity was divided into smaller parts in order to simplify the analysis. Chlorous acid self-decomposition was studied in the absence of transition metals (restricting path 3) and in the presence of a hypochlorous acid trapper (restricting path 4) [II]. The reaction between chlorous acid and hypochlorous acid (4) was studied under conditions where the rates of reactions (1-3) were insignificant [IV]. The rate parameters for iron-mediated chlorite decomposition (3) were determined against the experimental results of Fabian and Gordon (1992). The optimization of kinetic

parameters was carried out in each case with KinFit software (Jakobsson and Aittamaa 2005), applying a nonlinear curve fitting. The rate coefficient temperature dependencies were modeled with the Arrhenius equation. The progress of the reactions was computed by numerically integrating the initial value problem presented by the reaction rate equations and the initial solution composition. The experimentally monitored component concentrations were then compared to model predictions. The relative difference between the experimental and predicted values was squared, the squares were summed, and the summed value was used as the object function in optimization.

3.1 Chlorous acid self-decomposition

Chlorous acid self-decomposition (1) is one of the reaction paths assumed to consume chlorite during ClO_2 bleaching. The stoichiometry and kinetics of this reaction were studied in paper [II]. Chlorite and chlorous acid form an acid-base pair in aqueous solutions. Together they are referred to as chlorine (III), according to their oxidation state (Gordon et al. 1972). It was discovered that the reactive Cl(III) species is chlorous acid, while chlorite is stable. Reaction (2) speeds up Cl(III) decay in systems with notable acidity and chloride ion concentration. It was also found that even trace amounts of transition metals can speed up Cl(III) decay and alter the apparent stoichiometry. The effect of transition metals was highest around pH 2. EDTA was used to bind transition metals from the experiments that were used in parameter fitting procedures. The produced hypochlorous acid was prevented from reacting with Cl(III) by the introduction of dimethylsulphoxide (DMSO).

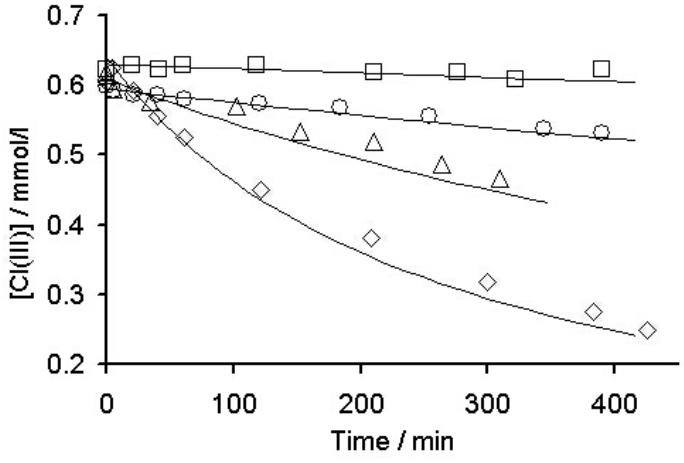

Figure 2. The decomposition of Cl(III) as a function of time at pH 2 at 40°C (□), 50°C (o), 60°C (Δ) and 70°C (◊). ($[Cl(III)]_0$ = 0.6 mM, $[DMSO]_0$ = 12 mM {hypochlorous acid trapping agent}, $[NaCl]_0$ = 5.16 mM and $[EDTA]_0$ = 10 mM). Bullets = experimental; lines = model prediction.

The self-decomposition reaction was found to follow second order kinetics with regards to $HClO_2$. The kinetics of reaction (2) was first order with respect to each reacting species. The reaction rate parameters for reactions (1) and (2) were fitted against the Cl(III) concentration data recorded in twelve experiments, in which the temperature (40, 50, 60, or 70°C), pH (1.0 or 2.0), and sodium chloride ion concentration (0, 5, 50, or 100 mM) were varied. The model system (reactions 1 and 2) corresponded well with the experimental results. An example comparison is shown in Figure 2. The rate parameters obtained and the comparison with previously reported rate coefficients are given in Table 1. The temperature dependency of the rate coefficients is reported for the first time in paper [II].

Table 1. The obtained rate parameters for reactions 1 and 2 and a comparison against literature values.

Reaction	[a]k (25°C)$_{\text{this work}}$	k (25°C)$_{\text{literature}}$	E_a/kJ/mol	ref
1	0.0021 $M^{-1}s^{-1}$	0.0055 $M^{-1}s^{-1}$	84	(Hong and Rapson 1968)
		0.0020 $M^{-1}s^{-1}$ (pH 1)		(Horvath et al. 2003)
		0.0018 $M^{-1}s^{-1}$ (pH 2)		(Horvath et al. 2003)
		0.0060 $M^{-1}s^{-1}$		(Kieffer and Gordon 1968a)
2	0.0027 $M^{-2}s^{-1}$	0.0018 $M^{-2}s^{-1}$	70	(Schmitz and Rooze 1981)
		0.0034 $M^{-2}s^{-1}$		(Horvath et al. 2003)
		0.0048 $M^{-2}s^{-1}$		(Hong and Rapson 1968)

[a] computed from the reaction rate coefficients (T = 55°C) and E_a-values obtained from regression

3.2 Fe-mediated chlorite decomposition

The Cl(III) self-decomposition experiments described in paper [II] revealed that in the absence of chelating agents, iron speeds up the Cl(III) decay rate and alters the product stoichiometry. The rate increase observed was substantial at around pH 2, but negligible at pH 1 or pH 3. Although the effect of iron was clearly seen, our experimental results were insufficient to make a thorough mechanistic analysis. There are, however, two reports that provide suitable experimental data as well as the mechanistic proposals for the iron-mediated Cl(III) reaction path (Fabian and Gordon 1992; Schmitz and Rooze 1985). In both cases, the in situ produced hypochlorous acid and its reactions with Cl(III) are involved in the mechanism. Any conclusions regarding the effect of iron are, hence, strongly influenced by the assumptions made with regards to hypochlorous acid. The assumptions made by Fabian and Gordon (1992) are anomalous and render the mechanistic proposition suspect [III]. Likewise, Schmitz and Rooze (1985) verified their model only qualitatively and left several rate parameters unspecified. The experimental results of Fabian and Gordon (1992) were used as regression data to determine the previously unknown rate parameters in the Schmitz and Rooze model.

The first step in the mechanism is an equilibrium reaction between the ferric ion (Fe^{3+}) and chlorite to generate chlorine dioxide and ferrous ion (Fe^{2+}) (5) (Fabian and Gordon 1992; Schmitz and Rooze 1984). The ferrous ion produces a chlorine monoxide radical (ClO) either with chlorous acid (6) or chlorite (7) (Schmitz and Rooze 1985; Ondrus and Gordon 1972; Fabian and Gordon 1991). Reactions (8-11) constitute a sequence of reactions where two radical species (Cl or ClO) either keep up the cycle by reacting with chlorous acid (8 and 9) or terminate the cycle by reacting with iron (10 and 11). Hypochlorous acid was assumed to react according to the scheme and parameters reported by Horvath et al. (2003) and Aieta & Roberts (1986b). The protolysis of Cl(III) and the hydroxylation equilibria of ferric ion (18-20) were also incorporated into the regression model.

$$ClO_2^- + Fe^{3+} \leftrightarrows ClO_2 + Fe^{2+} \quad (5)$$

$$HClO_2 + Fe^{2+} \rightarrow ClO\cdot + Fe(OH)^{2+} \quad (6)$$

$$ClO_2^- + Fe^{2+} + H_2O \rightarrow ClO\cdot + Fe(OH)_2^{+} \quad (7)$$

$$HClO_2 + ClO\cdot \rightarrow H^+ + ClO_3^- + Cl\cdot \quad (8)$$

$$HClO_2 + Cl\cdot \rightarrow HOCl + ClO\cdot \quad (9)$$

$$Cl\cdot + Fe^{2+} \rightarrow Cl^- + Fe^{3+} \quad (10)$$

$$ClO\cdot + Fe^{2+} \rightarrow ClO^- + Fe^{3+} \quad (11)$$

$$HClO_2 + HOCl \rightarrow Cl_2O_2 + H_2O \quad (12)$$

$$ClO_2^- + Cl_2 \rightarrow Cl_2O_2 + Cl^- \quad (13)$$

$$Cl_2O_2 + H_2O \rightarrow ClO_3^- + Cl^- + 2\,H^+ \quad (14)$$

$$Cl_2O_2 + ClO_2^- \rightarrow 2\,ClO_2\cdot + Cl^- \quad (15)$$

$$Cl_2O_2 + ClO_2^- + H_2O \rightarrow 2\,HOCl + ClO_3^- \quad (16)$$

Supporting equilibrium reactions

$$HClO_2 \leftrightarrows ClO_2^- + H^+ \quad (17)$$

$$Fe^{3+} + H_2O \leftrightarrows Fe(OH)^{2+} + H^+ \quad (18)$$

$$Fe^{3+} + 2\,H_2O \leftrightarrows Fe(OH)_2^{+} + 2\,H^+ \quad (19)$$

$$Fe^{3+} + 3\,H_2O \leftrightarrows Fe(OH)_{3\,(s)} + 3\,H^+ \quad (20)$$

The prediction of the present model is compared to the model of Fabian and Gordon and experimental results in Figures 3 and 4. Our model yields a very similar prediction to that of Fabian and Gordon. The curves from the two models coincide in Figure 3. The present model gives a better prediction for chlorine dioxide formation at a high Cl(III) concentration (Figure 4). The major benefit of our model is in the use of the widely-supported reaction scheme for hypochlorous acid.

The determined reaction coefficient values are shown in Table 2. The Cl and ClO radicals are very reactive and only the ratio of the parallel reaction rates (9/10) and (8/11) could be determined. The very small ratio k_9/k_{10} implies that the reaction rate (9) is insignificant and Cl radicals react almost exclusively with Fe^{2+}.

The reaction rate exhibits a significant fade-out after a rapid initial phase (Figure 3). This fade-out is not related to reactant extinction, since a significant Cl(III) residue remains in each experiment. Instead, the reaction slows down because of ClO_2 accumulation. The system is initially free of chlorine dioxide and the equilibrium in reaction (5) is far to the right-hand side. This provides the Fe^{2+} to initiate the chlorine radical reaction cycle. The accumulation of chlorine dioxide shifts the equilibrium gradually toward the left-hand side. This restricts the availability of Fe^{2+} and causes the rate to decrease. In bleaching applications, the chlorine dioxide would most probably be consumed in reactions with pulp constituents, allowing the Cl(III) depleting reaction to progress at a substantial rate.

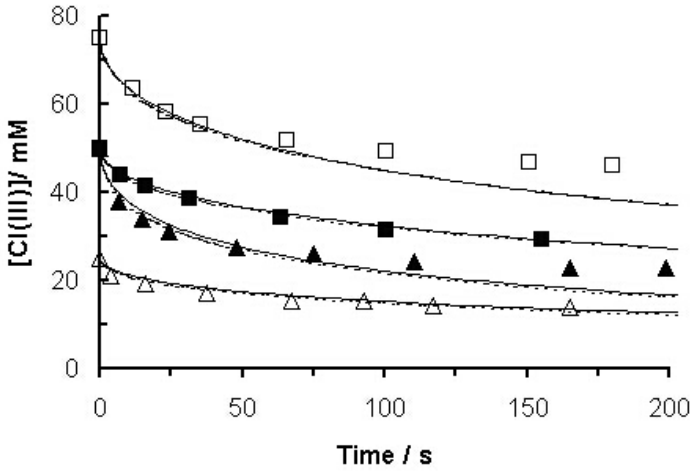

Figure 3. Fe-mediated Cl(III) decomposition: *bullets* – experimental, *solid line* – the model of this paper, *dashed line* - the model of Fabian and Gordon. Experimental data is provided by Fabian and Gordon (Fabian and Gordon 1992). (□) - $[Cl(III)]_0$= $7.50 \cdot 10^{-2}$ M, $[Fe^{3+}]$=$1.39 \cdot 10^{-3}$ M, pH=1.75; (■) - $[Cl(III)]_0$=$4.99 \cdot 10^{-2}$ M, $[Fe^{3+}]$=$1.39 \cdot 10^{-3}$ M, pH=1.25; (▲) - $[Cl(III)]_0$=$5.00 \cdot 10^{-2}$ M, $[Fe^{3+}]$=$4.20 \cdot 10^{-3}$ M, pH = 1.75; (Δ) -$[Cl(III)]_0$= $2.5 \cdot 10^{-2}$ M, $[Fe^{3+}]$=$1.39 \cdot 10^{-3}$ M, pH = 1.75

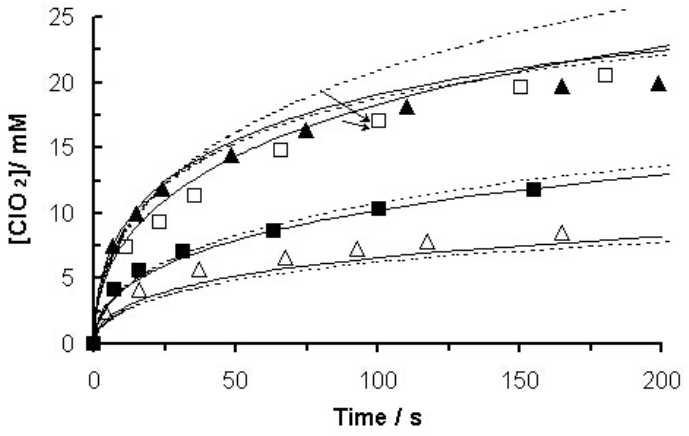

Figure 4. ClO_2 formation from Fe mediated Cl(III) decomposition: *bullets* – experimental, *solid line* – the model of this paper, *dashed line* - the model of Fabian and Gordon. Experimental data is provided by Fabian and Gordon (1992). (□) - $[Cl(III)]_0$= $7.50 \cdot 10^{-2}$ M, $[Fe^{3+}]$=$1.39 \cdot 10^{-3}$ M, pH=1.75; (■) - $[Cl(III)]_0$=$4.99 \cdot 10^{-2}$ M, $[Fe^{3+}]$=$1.39 \cdot 10^{-3}$ M, pH=1.25; (▲) - $[Cl(III)]_0$=$5.00 \cdot 10^{-2}$ M, $[Fe^{3+}]$=$4.20 \cdot 10^{-3}$ M, pH = 1.75; (Δ) -$[Cl(III)]_0$= $2.5 \cdot 10^{-2}$ M, $[Fe^{3+}]$=$1.39 \cdot 10^{-3}$ M, pH = 1.75

Table 2. Rate parameters for the Fe-mediated Cl(III) decomposition reactions.

Reaction	rate coefficient, k, at 25°C
5	k_5 = 269 $M^{-1}s^{-1}$ (Schmitz and Rooze 1985) $k_{5,\,rev}$ = $4.7 \cdot 10^5$ $M^{-1}s^{-1}$
14	k_6 = 930 $M^{-1}s^{-1}$ (Schmitz and Rooze 1985)
15	k_7 = 530 $M^{-1}s^{-1}$
8/11	$k_8 / k_{11} = 2.2 \cdot 10^{-4}$
9/10	k_9 / k_{10} = very small
Reaction	**equilibrium constant, K, at 25°C**
17	$K_{17} = 6.5 \cdot 10^{-3}$ M^1 (Dean 1999)
18	$K_{18} = 4.9 \cdot 10^{-7}$ M^1
19	$K_{19} = 1.6 \cdot 10^{-39}$ M^4

rev = reverse (rate coefficient for the reverse reaction)

3.3 Chlorate formation during chlorine dioxide delignification

The chlorate ion is one of the stable oxychlorine species formed during chlorine dioxide bleaching. It has been suggested that it is formed primarily through reactions involving chlorite and hypochlorous acid, but also directly from chlorine dioxide (Kolar et al. 1983; Fredricks et al. 1971). Chlorate formation is considered wasteful, as it is unable to facilitate the delignification reactions regardless of its high apparent oxidation power (valence +V) (Marpillero 1958; Rapson and Anderson 1977). It is also toxic to certain macro-brown algal species (Bergnor et al. 1987; van Wijk and Hutchinson 1995). Several reports deal with chlorate formation in delignification and bleaching (Rapson and Anderson

1977; Bergnor et al. 1987; Lindgren and Nilsson 1975; Nilsson and Sjostrom 1974; Rapson and Anderson 1978; Soila et al. 1962; Germgård et al. 1981; Ni et al. 1993; Yoon et al. 2004; Svenson et al. 2002; Svenson et al. 2006). A traditional way to study the chlorate formation mechanism is to conduct bleaching experiments under various conditions, record the chlorate yield, and use the observed dependencies to analyze and exclude the alternative reaction paths. The difficulty in this method is that the bleaching system constitutes an immense number of parallel and consecutively reactions, which are all more or less connected. Extracting the cause and effect relations in such systems is difficult. In paper [III] the topic was approached from another angle: the reaction rates and stoichiometries of potential chlorate-forming reactions were investigated through reaction kinetic modeling. A simplified depiction of the reaction system studied is shown in Figure 5. The potential of the individual paths was studied first. Then the reactions were combined and allowed to compete with each other. At this point, the model was augmented with reactions mimicking the bleaching environment. The model for chlorous acid self-decomposition was taken from paper [II] and that of iron-mediated chlorite decomposition was resolved in paper [III]. The HOCl-$HClO_2$ reaction scheme (12-16) in this study was adopted from the literature (Horvath et al. 2003; Aieta and Roberts 1986a). Our own experiments and mechanistic analyses regarding the HOCl-$HClO_2$ reactions were only conducted later.

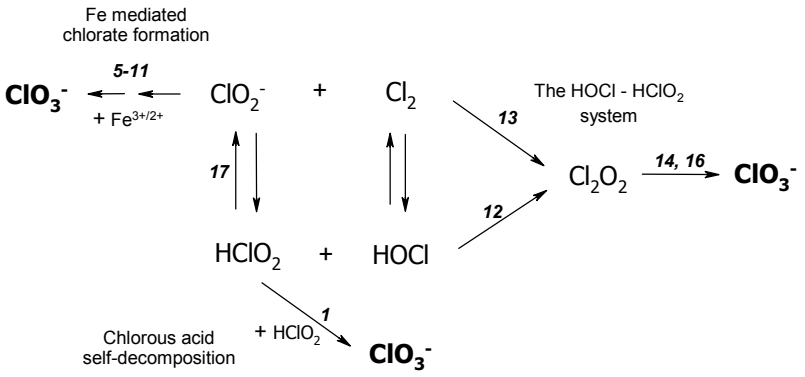

Figure 5. A simplified description of the chlorate-forming reaction paths (only the main reaction routes are shown).

3.3.1 Chlorous acid self-decomposition

The rate of chlorous acid self-decomposition (1) and the resulting chlorate formation were studied at 50°C, at a pH of 1.5-4 for a 60-min. reaction time. The reaction rate was found to be insignificant at pH 3.0 or above. Cl(III) conversion was observable at pH 2.5 and increased steadily as the pH was lowered further. Regardless of the accelerating effect of acidity, only about 70% of the Cl(III) reacted in one hour at pH 1.5. Experimental studies have shown Cl(III) consumption to be much faster in

delignification (Svenson et al. 2006). Hence, significant chlorate production via chlorous acid self-decomposition was considered unlikely at any pH.

3.3.2 The reaction between chlorous acid/chlorite and hypochlorous acid/chlorine

The reactions in this system (right-hand side in Figure 5) were completed in less than ten seconds irrespective of the reaction conditions. The stoichiometric examinations were hence made from the final composition of the reaction solution. The reaction stoichiometry was found to depend on several factors: chloride ion concentration, Cl(III) concentration, and pH. Chlorate formation was substantial in any case, suggesting that this reaction path is a potential contributor to chlorate production in pulp delignification. Chlorate production was reduced both by increasing the chloride ion concentration and pH. The effect of pH was, however, quite small between pH 2.5 and 4. The effect of chloride ions was remarkable: raising the chloride ion concentration from 1 to 5 mM led to a reduction in chlorate formation of roughly 30%.

3.3.3 Chlorate formation through radical chemistry

The rate of Fe-mediated Cl(III) decomposition and the related chlorate formation are shown in Figure 6. The effect of pH is dramatic: the rate is insignificant at pH levels of 3.5 and 4.0 and still very slow at pH 3.0, but even at pH 2.5 more than 95% of the initial Cl(III) reacts within 60 minutes. The rate exhibits a maximum between pH 1.5-2.0. In the heavily acidic region (pH < 1.5), the rate declines again. Chlorate production is negligible above pH 3, but at pH 2.5 or below the yield is around 25-35% of the available Cl(III). The other stable chlorine-containing products, hypochlorous acid and chloride ion, were produced in a ratio of approximately 1:1 irrespective of the pH.

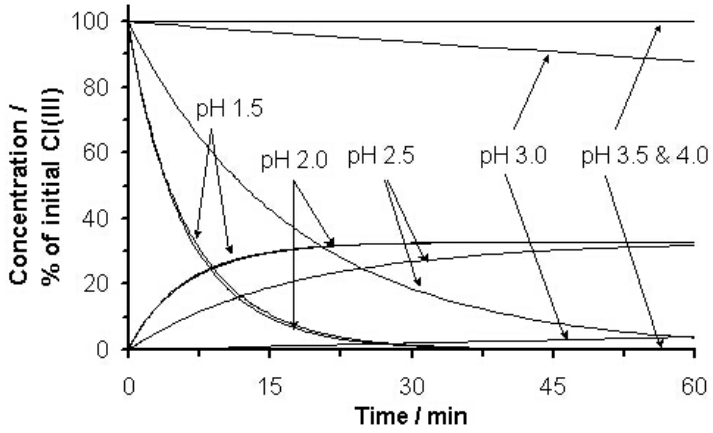

Figure 6. The effect of pH on Fe-mediated Cl(III) decomposition and the related chlorate formation. Curves starting from 0% represent chlorate concentrations and those starting from 100% represent Cl(III) concentrations. T = 50°C, $[Cl(III)]_{initial}$ = 8 mM, $[Fe]_{tot}$ = 20 μM.

3.3.4 Total chlorate production in delignification

The total chlorate formation was predicted in simulations where the reactions were allowed to compete with each other, as well as with the reactions assumed to contribute to Cl(III) consumption or affect the chlorate-forming reactions in real delignification systems. The predicted chlorate formation is shown in Figure 7. The individual reaction route simulations suggested that the rate of chlorous acid self-decomposition was too slow to compete against the other routes at any investigated pH. This was confirmed in the overall system simulations.

The results suggest that at pH below 3 chlorate formation results from both Fe-mediated Cl(III) decomposition and through the HOCl-$HClO_2$ system. At pH above 3, only the latter route has the kinetic prerequisites to produce chlorate. The total production simulations showed an increasing chlorite residue at pH 3 and above. This indicates that an increasing pH decelerates the rate-determining step in the HOCl-$HClO_2$ system and allows the hypochlorous acid to be consumed to an increasing extent in organic reactions. This finding is in accordance with experimental observations (Kolar et al. 1983; Rapson and Anderson 1978; Yoon et al. 2004; Svenson et al. 2006).

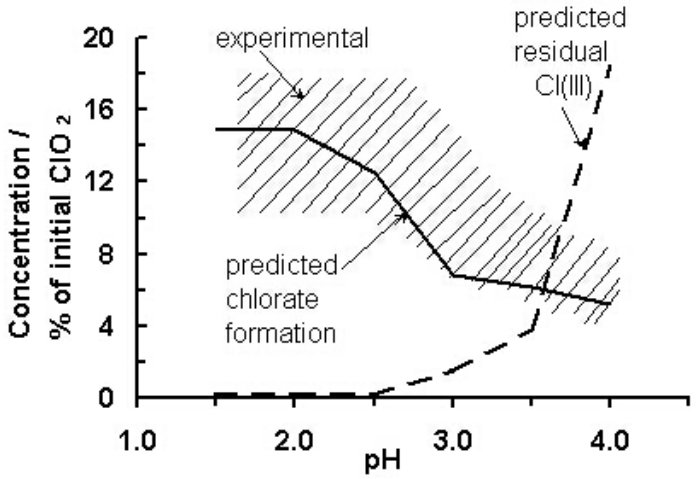

Figure 7. Total chlorate production as a function of pH. The diagonal bars indicate the range of experimental observations (Kolar et al. 1983; Ni et al. 1993; Svenson et al. 2006; Medina et al. 2008). Simulation conditions: reaction time = 45 min, T = 50°C, $[Cl(III)]_{initial}$ = 8 mM, $[Cl^-]_{initial}$ = 1 mM.

It was also observed that reaction (2) had no practical importance regarding the simulation result at any tested pH (1.5-4.0). Excluding reaction (2) from the simulations changed the final composition by less than 0.1%. The effect was insignificant, even when the chloride ion concentration was increased to 10 mM. Clearly, reaction (2) would have required a much higher acidity, temperature, and/or a higher chloride ion concentration to have an impact.

3.4 Reaction between hypochlorous acid and chlorous acid

The $HOCl$-$HClO_2$ reaction mechanism was first considered by Taube and Dodgen (Taube and Dodgen 1949) and it has been examined further in numerous subsequent reports (Fabian and Gordon 1992; Hong and Rapson 1968; Horvath et al. 2003; Kieffer and Gordon 1968a; Schmitz and Rooze 1981; Schmitz and Rooze 1985; Kieffer 1967; Kieffer and Gordon 1968b; Peintler et al. 1990; Emmenegger and Gordon 1967; Jia et al. 2000; Gordon and Tachiyashiki 1991). A dichlorine dioxide anhydride (Cl_2O_2) is formed in the first step (12). It is consumed in two or more reactions yielding chlorine dioxide, chloride, and chlorate as the stable final products (14-16, 21). Reaction (12) is considerably slower than the subsequent Cl_2O_2-consuming reactions. Hence, in the overall reaction, step (12) is rate-limiting and the relative rates of the Cl_2O_2-consuming paths dictate the observed stoichiometry. The reported mechanistic alternatives and rate coefficients are gathered in Table 3.

Table 3. The reaction steps and rate coefficients (25°C) reported for the $HOCl$-$HClO_2$ overall reaction.

Reaction	reference →	TD	HR	P	GT	FG	J	H
		[a] Reaction rate coefficient						
12	$HClO_2 + HOCl \rightarrow Cl_2O_2 + H_2O$	[inc]	[b] 30	[c] $2\cdot10^4$	$1\cdot10^5$	[inc]	1.6	[inc]
14	$Cl_2O_2 + H_2O \rightarrow 2\,H^+ + Cl^- + ClO_3^-$	[inc]	[inc]	[d] $9.3\cdot10^3$	-	$1\cdot10^7$	-	$(1\cdot10^3 + 2.85\cdot10^5\,[Cl^-])$
14'	$Cl_2O_2 + OH^- \rightarrow H^+ + Cl^- + ClO_3^-$	-	-	-	-	-	$1.3\cdot10^{12}$	-
15	$Cl_2O_2 + ClO_2^- \rightarrow 2\,ClO_2 + Cl^-$	-	[inc]	$5\cdot10^8$	-	$5\cdot10^8$	$1\cdot10^7$	$(2.01\cdot10^7 + 8.4\cdot10^9\,[Cl^-])$
16	$Cl_2O_2 + ClO_2^- + H_2O \rightarrow 2\,HOCl + ClO_3^-$	-	-	-	-	-	$1\cdot10^{11}\,[H^+]$	$1.11\cdot10^7$
21	$2\,Cl_2O_2 \rightarrow 2\,ClO_2 + Cl_2$	[inc]	-	-	-	-	-	-

TD = Taube and Dodgen 1949, HR = Hong and Rapson 1968, P = Peintler et al. 1990, GT = Gordon and Tachiyashiki 1991, FG = Fabian and Gordon 1992, J = Jia et al. 2000, H = Horvath et al. 2003

[a] the dimensions of first, second, and third order rate coefficients are s^{-1}, $M^{-1}s^{-1}$, and $M^{-2}s^{-1}$, respectively

[b] the rate coefficient is computed from reported experimental results using $k_{23} = 1.8\cdot10^4\ M^{-2}s^{-1}$ (Wang and Margerum 1994).

[c] the rate coefficient is computed from reported experimental results using $K_{a,17} = 1.1\cdot10^{-2}$ M (Fabian 2001).

[d] k_{14}/k_{15} is given in the original report, $k_{15} = 5\cdot10^8$ is assumed here

inc = the reaction is included in the mechanism; rate coefficients are not reported

- = the reaction is not included in the mechanism

The presently available kinetic data has been obtained either under highly acidic (Fabian and Gordon 1992; Hong and Rapson 1968; Horvath et al. 2003; Schmitz and Rooze 1981; Taube and Dodgen 1949), close to neutral (Jia et al. 2000), or mildly alkaline conditions (Gordon and Tachiyashiki 1991). The industrial chlorine dioxide bleaching processes are conducted in a mildly acidic environment (pH 2-5). Thus, none of the existing models can be directly applied to simulate the reactions in the bleaching environment. Extrapolation is also ambiguous, for the reported rate coefficients vary within 5 orders of magnitude (Table 3), the rate expression may involve chlorous acid or chlorite ion (Jia et al. 2000), and the proposed Cl_2O_2 reaction schemes are diverse. Consequently, experiments were

conducted under mildly acidic conditions and the results were used in analyzing the reaction kinetics and mechanism.

3.4.1 Experimental setup and modeling principles

The reaction kinetics and stoichiometry were studied at pH = 2.5 – 4.7 with a temperature of either 5, 15, or 25°C. External buffer compounds were not used, as they are reported to interfere with the reactions (Jia et al. 2000), and the applied parameter regression method did not require a constant pH. The pH range applied ensured that the reaction rates of iron-mediated chlorite decomposition (5-11) and chlorous acid self-decomposition (1) were insignificant [III]. Samples were taken at regular intervals and treated with DMSO to terminate the reaction (immediate consumption of residual HOCl). Chlorine dioxide, chlorite, and chlorate were determined from the samples using iodometric titration (Wartiovaara 1982).

Table 4. Experimental reaction conditions and initial solution compositions used in the $HClO_2$-HOCl experiments.

Exp. Series	$[Cl(III)]_0$ /mM	$[HOCl]_0$ /mM	$[ClO_3^-]_0$ /mM	$[Cl^-]_0$ /mM	T / °C	Initial pH [a]	End pH
1	0.60	0.17	0.04	0.16	25	3.0	3.2
2	0.61	0.20	0.04	0.16	16	3.0	3.3
3	0.62	0.16	0.05	0.16	5.5	3.0	3.3
4	0.60	0.16	0.05	0.16	5.6	2.5	2.7
5	0.60	0.16	0.05	0.16	7.0	3.5	4.7
6	0.62	0.16	0.05	1.16	5.4	3.0	3.3
7	0.61	0.15	0.05	3.16	5.8	3.0	3.2
8	1.19	0.18	0.07	0.32	5.0	3.0	3.2
9	0.59	0.17	0.05	0.16	25	3.5	4.7
10	0.52	0.16	0.05	1.16	6.7	3.5	4.4
11	0.59	0.17	0.04	3.16	6.9	3.5	4.4

[a] The initial pH was computed from solution composition.

Reactions (13, 17, 22 and 23) were incorporated into the model to obtain a comprehensive description for the whole reaction system. Reaction (13) provides an alternative route for Cl_2O_2 formation (Aieta and Roberts 1986b; Taube and Dodgen 1949; Peintler et al. 1990; Emmenegger and Gordon 1967; Nicoson and Margerum 2002) and reactions (22) and (23) represent the reversible hydrolysis of chlorine. The rate parameters of Aieta and Roberts (1986b), $k_{13} = 1.6 \cdot 10^4$ $M^{-1}s^{-1}$ at 25°C and $E_{a,13}$ = 39.9 kJ/mol, were adopted for reaction (13). The full reaction system is depicted in Figure 8.

$$Cl_2 + H_2O \rightarrow HOCl + H^+ + Cl^- \quad (22)$$

$$HOCl + H^+ + Cl^- \rightarrow Cl_2 + H_2O \quad (23)$$

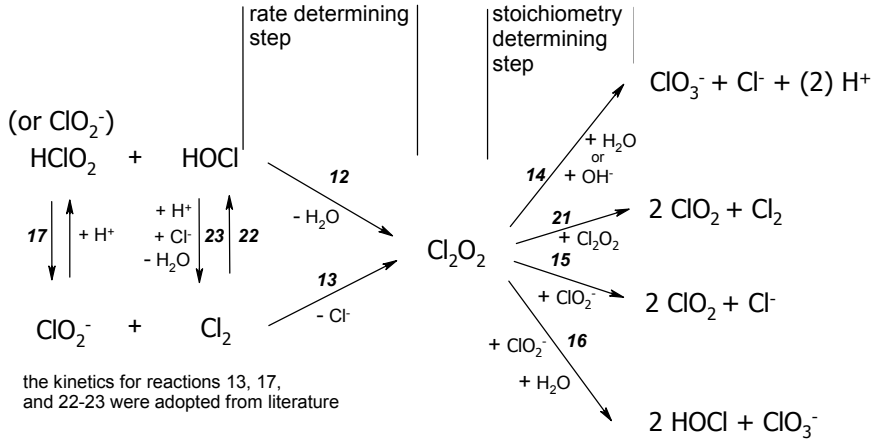

Figure 8. A schematic representation of the reaction steps involved in the HOCl – $HClO_2$ system.

3.4.2 Effect of temperature, pH, and solution composition on reaction rate and stoichiometry

The temperature increased the reaction rate and promoted chlorate formation over chlorine dioxide. The reaction rate increased also with acidity, but pH had no effect on the overall stoichiometry. The chloride ion concentration was found to have a dramatic influence both on reaction rate and stoichiometry. The chloride ion concentration was varied by introducing either 1.0 or 3.0 mM of sodium chloride into the reaction solution. Increases in chloride ion concentration resulted in a higher reaction rate and lower chlorate production. A higher initial Cl(III) concentration sped up the reaction, but had no apparent effect on the reaction stoichiometry. In conclusion: the rate-determining step was affected by temperature, pH, chloride, and initial Cl(III) concentration, whereas the overall stoichiometry was changed only by temperature and the chloride ion concentration.

3.4.3 Kinetic and mechanistic analysis

First, the possible applicability of the earlier models in reproducing the experimental findings was tested. The experimental Cl(III) decomposition rate at pH 3 and T = 5.5°C is compared to predictions produced using the earlier models in Figure 9. The predicted rates are either substantially too slow or too fast. Figure 9 also shows a prediction where the rate of reaction (12) is set to zero and where the Cl(III) depletion thus results only from the reaction between the chlorine and chlorite (13). The predicted depletion rate is substantially too slow, indicating that reaction (12) is important in the present system.

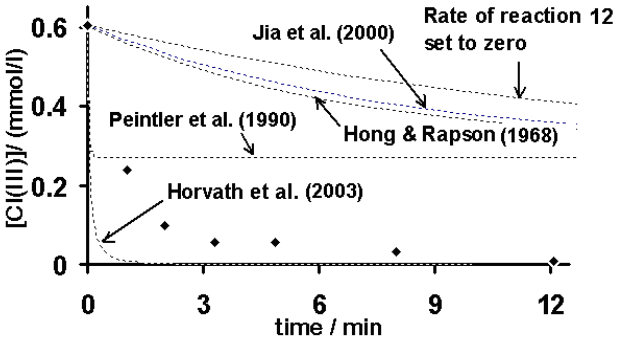

Figure 9. The predicted Cl(III) depletion using previously reported kinetic models. A case where r_{12} is completely omitted is also shown. Prediction (dotted line), experiment series 3 (bullets), T = 5.5°C, initial pH ≈ 3.0.

The predictions using our model are fully presented and compared to the experimental results in paper [IV]. Overall, the model produced good predictions. An example comparison is given in Figure 10. The reactions and rate parameters in use are given in Table 5. The rate coefficient and the activation energy obtained for reaction (12) are $k_{12} = 406\ M^{-1}s^{-1}$ and $E_{a,12} = 54$ kJ/mol. The rate coefficient value is more than one order of magnitude smaller than has been reported for the parallel reaction between chlorine and chlorite (13) (Table 5). This is in accordance with observations that Cl(III) reacts faster with elemental chlorine than with hypochlorous acid (Emmenegger and Gordon 1967). This is also in agreement with our own finding that NaCl additions accelerate the observed Cl(III) decay: a higher chloride ion concentration shifts the equilibrium between the chlorine and hypochlorous acid toward the former, and thereby promotes the faster route (13) that involves chlorine (Figure 8).

In the stoichiometry-determining step, rate parameters were identified only for reactions (15) and (16) (Table 5). The Cl_2O_2-consuming reactions are extremely fast (Horvath et al. 2003; Peintler et al. 1990), and consequently only the ratio of reaction rates r_{15} and r_{16} could be determined. Reaction (15) is strongly catalyzed by chloride ions and the apparent rate coefficient, k_{15}, involves chloride ion concentration. The inhibiting effect of the chloride ions observed on chlorate formation was very strong: even a millimolar level chloride ion concentration is enough to prevent chlorate production almost completely (Figure 10). This suggests that in pulp bleaching applications, chlorate production through this path could be suppressed through control of the chloride ion concentration in the suspension.

Successful reproduction of the experimental results required inclusion of reaction (23) in the regression, the formation of elemental chlorine from hypochlorous acid and chloride. The literature value for k_{23} resulted in a poor prediction of reaction rate changes related to chloride ion concentration. The k_{23} value obtained is somewhat higher, but of the same order of magnitude as the

values determined in earlier studies (Aieta and Roberts 1986a; Wang and Margerum 1994; Connick and Chia 1959; Eigen and Kustin 1962). In principle, the poor prediction of rate changes related to chloride ion concentration could also have resulted from too low a rate of reaction (13). However, including reaction (13) in the regression did not result in better predictions. If reaction rate r_{13} was manually elevated (hypothetical sensitivity analysis), the overall Cl(III) conversion rate did not increase, but only the maximum concentration of elemental chlorine was reduced. This indicates that between the consecutive reaction steps (23) and (13), the first was rate-limiting.

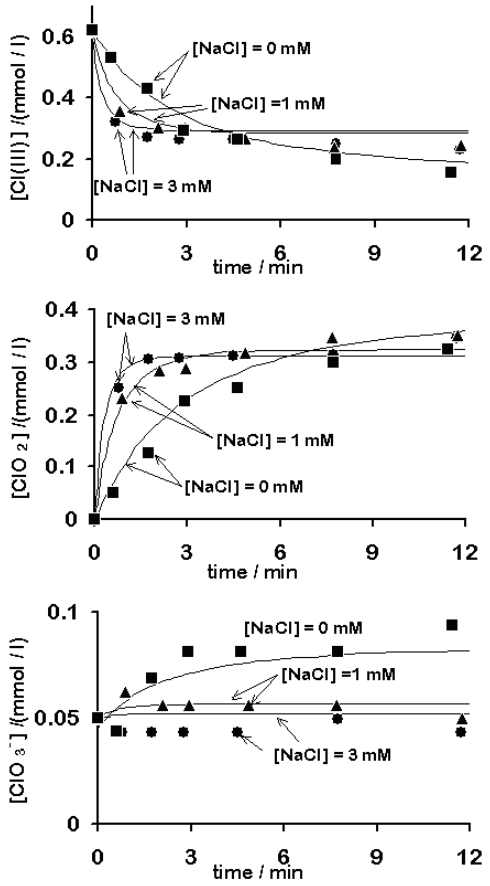

Figure 10. The effect of sodium chloride concentration on (A) Cl(III) depletion, (B) chlorine dioxide formation, and (C) chlorate formation. Experiment series 3, 6, and 7, T ≈ 5°C, initial pH_0 ≈ 3.0, bullets = experimental, line = model prediction.

Table 5. The reactions and rate parameters for the HOCl-$HClO_2$ system. Normal letters are used for parameters obtained from regression and italics for literature parameters. Parameter intervals represent 95% confidence limits using student T distribution.

Reaction		k (at 12°C)	E_a / (kJ/mol)
12	$HOCl + HClO_2 \rightarrow Cl_2O_2 + H_2O$	406 ± 93 $M^{-1}s^{-1}$	54 ± 13
13	$Cl_2 + ClO_2^- \rightarrow Cl_2O_2 + Cl^-$	*$1.0 \cdot 10^4$ $M^{-1}s^{-1}$* (Aieta and Roberts 1986b)	*39.9*
15	$Cl_2O_2 + ClO_2^- \rightarrow 2\ ClO_2 + Cl^-$	[a] $1 \cdot 10^{11} \cdot [Cl^-]$ $M^{-2}s^{-1}$	[a] 50
16	$Cl_2O_2 + ClO_2^- + H_2O \rightarrow 2\ HOCl + ClO_3^-$	$6.25 \pm 0.75 \cdot 10^6$ $M^{-1}s^{-1}$	78 ± 6
17	$HClO_2 \leftrightarrows ClO_2^- + H^+$	[a] *$K_{a,17} = 1.4 \cdot 10^{-2} M^{-1}$* (Dean 1999)	
22	$Cl_2 + H_2O \rightarrow HOCl + H^+ + Cl^-$	*$6.7\ s^{-1}$* (Wang and Margerum 1994)	*63*
23	$HOCl + H^+ + Cl^- \rightarrow Cl_2 + H_2O$	$5.0 \pm 2.0 \cdot 10^4$ $M^{-2}s^{-1}$	[ni]

[ni] = the value was too small to be identified
[a] a fixed parameter, value taken from (Horvath et al. 2003).
[b] from thermodynamic constants (temperature dependency included)

4 CHLORINE DIOXIDE DELIGNIFICATION MODEL

The results from our oxychlorine reaction studies in an aqueous solution were combined with literature knowledge regarding the essential organic reaction paths to obtain a chemistry model of chlorine dioxide delignification. The chemistry model was further combined with the phenomenon-based pulp suspension model (chapter 2, paper II) to obtain a ClO_2 delignification model [V]. Documented thermochemical and reaction rate parameters were exploited as much as possible. The unknown rate parameters were obtained by comparing the predictions with experimental laboratory-scale results (O-delignified birch pulp) reported by Lehtimaa et al (2010a, 2010b). The model predictions were used to analyze the suitability of individual theories and the hypothesis, as well as evaluating how well the present model is able to reproduce the experimental results.

4.1 Chemistry models

A full list of all the incorporated chemical reactions and rate parameters is given in the Appendix of paper [V]. The list is not assumed to contain all conceivable reactions that may take place during delignification, but is offered as a simplified model for the essential reaction paths.

4.1.1 Lignin reactions

The unreacted residual lignin, either phenolic or non-phenolic, is modeled with phenyl propane units. The reaction between chlorine dioxide and unreacted (primary) lignin is assumed to proceed via three parallel paths (Figure 11). The reaction produces a quinone (Lindgren 1971; Ni et al. 1994; Brage et al. 1991a; Dence et al. 1962; Wajon et al. 1982; Gunnarsson and Ljunggren 1996), a muconic acid ester/the corresponding lactone (Lindgren 1971; Ni et al. 1994; Brage et al. 1991a; Dence et al. 1962; Gunnarsson and Ljunggren 1996; Brage et al. 1991b; McKague et al. 1994; McKague et al. 1995), and a reactive intermediate (path C). The first two compounds have been identified as direct oxidation products of lignin model compounds. Path (C) accounts for the experimental findings that a significant part of lignin is degraded beyond the level of quinones and muconic acids (Ni et al. 1994; Brage et al. 1991a; McKague et al. 1994). The structure of the reactive intermediate is unknown and it is depicted here as a non-esterified muconic acid merely to indicate the level of oxidation. The relative importance of reaction paths A-C depends on the detailed structure of the lignin substrate (Ni et al. 1994; McKague et al. 1994; McKague et al. 1995). In the model, the reaction paths are assumed to proceed in a 1:1:2 ratio (A:B:C), resembling the proportions reported for vanillyl alcohol (Ni et al. 1994).

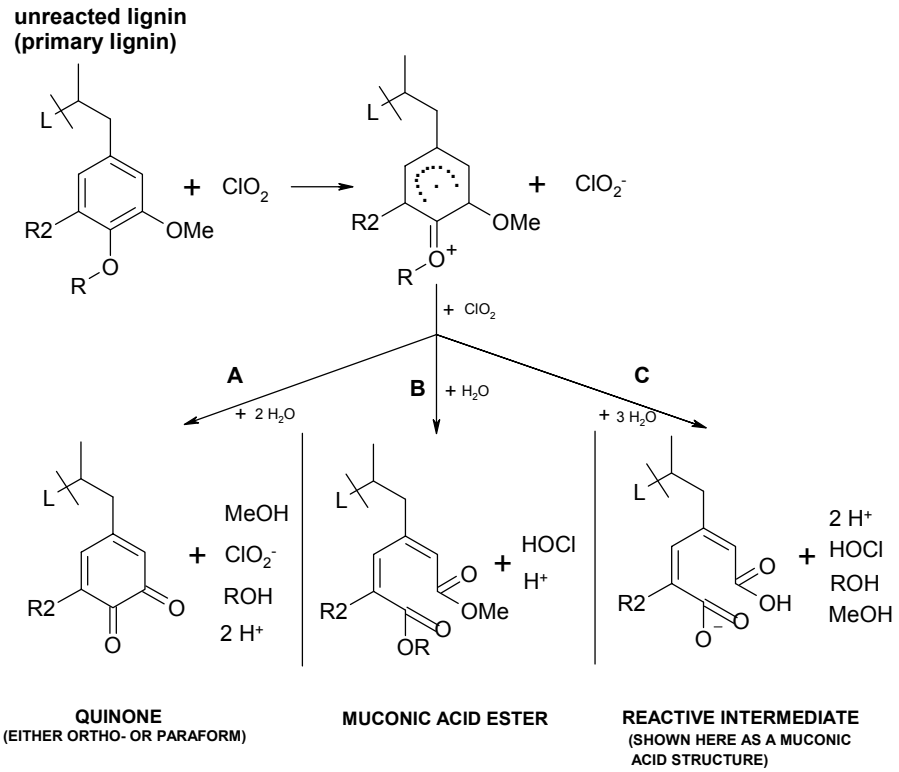

Figure 11. The oxidation of unreacted lignin by chlorine dioxide. (R2 = H for guaiacyl lignin, R2 = OMe for syringyl lignin; R = H for phenolic lignin, R = Lignin for non-phenolic lignin)

The reactions depicted in Figure 11 concern both phenolic and non-phenolic lignin. The reaction kinetics for phenolic lignin is defined according to the oxidation rate of 2-methoxyphenol ($k_{dissociated}$ = $1 \cdot 10^9$ $M^{-1}s^{-1}$, $k_{undissociated}$ = $1 \cdot 10^3$ $M^{-1}s^{-1}$) (Hoigne and Bader 1994). The rate parameters reported for other phenols are of a similar magnitude (Wajon et al. 1982; Hoigne and Bader 1994). The rate of non-phenolic lignin oxidation is adopted from Brage et al. (Brage et al. 1991a). Chlorine substituents are believed to cause steric hindrance and retard the oxidative cleavage of ether bonds (Dence and Reeve 1996). The reactive intermediate structure produced from primary lignin (Figure 11) is assumed to yield maleic acid (McKague et al. 1994; McKague et al. 1995), which reacts further to give a highly fractionated, fully-saturated lignin derivative. All lignin reactions are assumed to proceed similarly in the fiber wall and in the liquor, i.e. the same reaction routes and kinetics apply for the lignin pseudo-components in liquor (dissolved) or in the fiber wall (insoluble). Syringyl and guaiacyl lignin units are distinguished with regard to molar weight; their reaction paths and kinetics are assumed to be equal.

Hypochlorous acid is assumed to chlorinate phenols (Wajon et al. 1982; Soper and Smith 1926; Rebenne et al. 1996; Deborde and von Gunten 2008) and to generate new phenolic groups. The chlorination of non-phenolic lignin by hypochlorous acid is assumed to be insignificant, because

aromatic compounds without specific substituents are known to react slowly with HOCl (Voudrias and Reinhard 1988). The generation of phenolic groups is incorporated based on implications from experimental work (Ni et al. 1995; Joncourt et al. 2000).

Chlorine is known to both chlorinate and oxidize lignin (Dence and Reeve 1996). Chlorination experiments have indicated that the C_9-lignin units become monochlorinated almost instantaneously (Ni et al. 1990). Thus, chlorination is assumed to occur one order of magnitude faster than oxidation. The absolute values of the reaction rate parameters were obtained from regression. The chlorination reactions are assumed to yield only monochlorinated compounds (Dahlman et al. 1994).

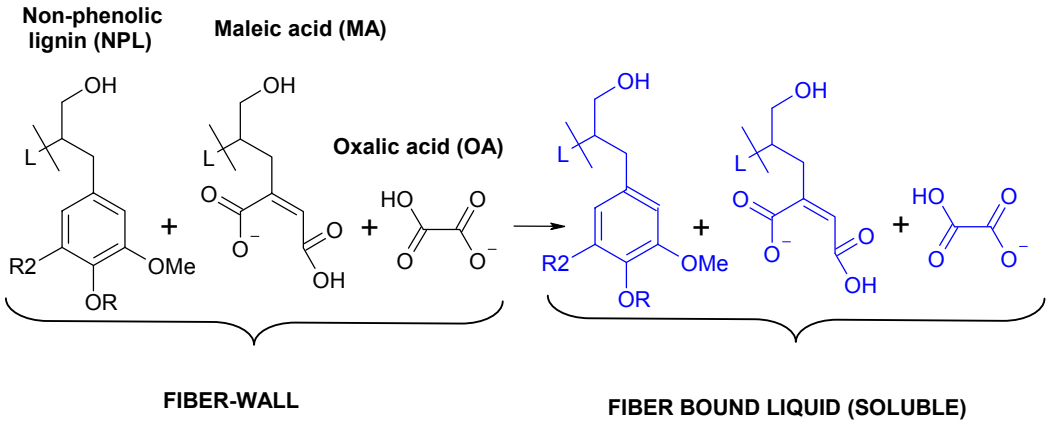

$$\textbf{dissolution rate} = -\frac{\mathbf{d[NPL]_{FIBER}}}{\mathbf{dt}} = -\frac{\mathbf{d[MA]_{FIBER}}}{\mathbf{dt}} = -\frac{\mathbf{d[OA]_{FIBER}}}{\mathbf{dt}}$$
$$= \frac{\mathbf{d[NPL]_{FBL}}}{\mathbf{dt}} = \frac{\mathbf{d[MA]_{FBL}}}{\mathbf{dt}} = \frac{\mathbf{d[OA]_{FBL}}}{\mathbf{dt}} = \mathbf{k \cdot [NPL]_{FIBER} \cdot [MA]_{FIBER}}$$

Figure 12. An example of a lignin dissolution reaction.

Lignin dissolution is modeled as a transfer process of compounds from the insoluble fiber wall into the fiber-bound liquid. The macromolecular nature of the lignin is taken into account in the dissolution reactions of lignin. The following principles were used in the lignin dissolution scheme: (i) the dissolution is directly proportional to the concentration of fragmented and hydrophilic (carboxylic acids) lignin structures, and (ii) the dissolving entity ("lignin fragment") is a sum of monomeric units, which dissolve at equal rates. An example of a lignin-dissolving reaction and the dissolution rate equation is given in Figure 12. The oxidative reactions of ClO_2 and other oxychlorine species increase fragmentation and hydrophilicity of residual lignin and force some of the lignin to dissolve. The assumption is that the hydrophilic lignin derivatives are attached to the other lignin units and hence

they also force some unreacted lignin to dissolve. The rate of each dissolution reaction is proportional both to the concentration of the fragmented/hydrophilic lignin derivative and the unreacted lignin unit. The more extensively degraded lignin derivatives dissolve a larger fraction of unreacted structures, and vice versa. Guidelines for choosing the dissolution stoichiometry (the ratio of fragmented/hydrophilic lignin derivatives to the primary lignin units) were adopted from studies dealing with dissolved D0-stage lignin (Dahlman et al. 1995; Vilen et al. 2000; Österberg and Lindström 1985).

4.1.2 Reactions regarding other pulp and liquor components

Hypochlorous acid and chlorine react with hexenuronic acid (Costa and Colodette 2007; Juutilainen et al. 1999), producing various chlorinated and unchlorinated degradation products. The reaction scheme was formulated so that a lower pH increases the proportion of chlorinated degradation products, and vice versa. The correlation between pH and the fraction of chlorinated HexA products has been observed in experimental work (Vuorinen et al. 1997).

Chlorine dioxide reacts with unsaturated sterols and fatty acids (Freire et al. 2003). Both reactions yield unchlorinated products. Reports state that both sitosterol and unsaturated fatty acids are removed to a very high extent during ClO_2 delignification (Jansson et al. 1995). Hence, the rate coefficients were set to a value ($k = 10\ M^{-1}s^{-1}$), ensuring rapid depletion. The chlorination of extractives was omitted, since it has been reported that extractive components make only a minor contribution to both OX and AOX during the chlorine dioxide delignification of birch kraft pulp (Björklund et al. 2004).

The inorganic oxychlorine reaction scheme covers the essential reaction paths depleting Cl(III) and producing chlorate, i.e. chlorous acid self-decomposition [II], iron-mediated chlorite depletion [III], the interaction between chlorous acid and hypochlorous acid [IV], and the reversible hydrolysis of chlorine (Wang and Margerum 1994).

4.1.3 Protolysis reactions and other equilibrium reactions

The protolysis coefficients of chlorous acid and hypochlorous acid were computed from thermochemical constants [I]. The equilibrium coefficients for iron(III) hydroxylation were computed in a similar manner. This procedure takes into account the temperature dependency of the dissociation coefficients. Lignin-related phenols generally dissociate at around pH 9-11 (Ragnar et al. 2000; Norgren and Lindström 2000a). The pK_a value reported for kraft lignin phenols (0.1 M NaCl), including the temperature dependency of the dissociation coefficient, is assigned for phenolic lignin (Norgren and Lindström 2000a). The value at 50°C is $pK_{a,phenolic\text{-}lignin} = 10.1$. Chlorine substituents are

said to decrease the pK_a value of phenols by approximately one unit (Hoigne and Bader 1994). Thus, chlorinated phenolic lignin is defined to have a pK_a value of one unit smaller than its unchlorinated equivalent. The value at 50°C is $pK_{a,phenolic\text{-}lignin\text{-}Cl} = 9.1$. The protolysis coefficients for maleic acid (Dean 1999), oxalic acid (Dean 1999), hexenuronic acid (Teleman et al. 1995), and methyl-glucuronic acid (Teleman et al. 1995) are defined according to the corresponding real compound values at 25°C. The temperature dependency of hexenuronic and methyl-glucuronic acid dissociation coefficients is estimated using the enthalpy of dissociation (-3 kJ/mol) reported for uronic acids in kraft pulp fibers (Lindgren et al. 2001).

4.2 Model validation

The model predictions were compared to kappa number, hexenuronic acid, inorganic oxychlorine compound, and organochlorine (AOX, OX) measurements at several time points during five delignification experiments. Laboratory-scale delignifications were done with Finnish oxygen-delignified birch kraft pulp. A complete description of the experimental procedures and results is given by Lehtimaa et al (2010a, 2010b).

4.2.1 Kappa number model

The comparisons with the experimental results regarding lignin structures and organochlorine formation could not be done on molecular scale, as reliable analytical methods for detailed characterization of the residual and dissolved lignin were not available. Instead, the simulation results were converted into standardized bulk variables - kappa number, AOX, OX, and COD – in order to make the evaluation. Equation (e5) was used to give the connection between the kappa number, residual lignin content (w-%), and hexenuronic acid content (Li and Gellerstedt 1997). Equation (e5) was solved for κ to compute the kappa number from the molecular scale composition (e6). All the unsaturated lignin pseudo-compounds were assumed to make specific contributions to the kappa number. Thus, the lignin content, L, in (e6) was handled as a proportioned summation term given in (e7). Reported permanganate consumptions of lignin-model compounds (Li and Gellerstedt 1998; Brogdon 2001; Li et al. 2002; Hamzeh et al. 2005) were used to define the 'oxidation equivalent' (OxEq) values for each unsaturated lignin pseudo-compound (Table 6). The kappa contribution of the extractive components was incorporated through the summation term as well. The sterol and fatty acid pseudo-compounds were assigned the oxidation equivalent reported for an unconjugated double bond (Li and Gellerstedt 1998). The proportionality factor ($OxEq_i$/ $OxEq_{arom}$) in (e7) is unity for the unreacted lignin (full aromatic ring) and less than unity for the oxidized lignin pseudo-compounds and extractives. Compounds in the solid fiber wall and in the fiber-bound liquid contribute to the computational kappa number. Compounds in the external liquid are omitted.

$$L = (\kappa - H \cdot 0.086) \cdot 0.15 \quad \text{(e5)}$$

$$\kappa = L / 0.15 + H \cdot 0.086 \quad \text{(e6)}$$

$$L = 100\% \cdot \sum_i \left(\frac{OxEq_i}{OxEq_{arom}} \cdot M_{w,i} \cdot c_i \right) / 1000 \quad \text{(e7)}$$

where L = lignin content (weight %)

κ = kappa number

H = hexenuronic acid content (mmol/kg)

$M_{w,i}$ = molar weight of component i (g/mol)

c_i = component concentration (mol/kg fiber)

$OxEq_i$ = oxidation equivalent value of component i

$OxEq_{arom}$ = oxidation equivalent value of full aromatic ring

Table 6. The oxidation equivalent values assigned for the lignin and extractive pseudo-compounds.

Pseudo-compound	Reported $KMnO_4$ oxidation equivalents [a]	Assigned oxidation equivalent value
Full aromatic ring (phenolic and non-phenolic lignin)	12-19.6	16
Quinone	6.8-12.5	10
Muconic acid	10.8-14.3	12
Maleic acid	10-11.7	11
Sterols	-	5.7
Unsaturated fatty acids	-	5.7

[a] (Li and Gellerstedt 1998; Brogdon 2001; Li et al. 2002; Hamzeh et al. 2005)

4.3 Organochlorine content and chemical oxygen demand models

The AOX and OX values were computed by summing up the concentrations of all the chlorine-containing compounds in the external liquid (AOX) or in the solid fiber wall (OX), and proportioning the values to the unit mass of dry fibers. Monochlorinated compounds were assumed to contribute with a factor of 1 and dichlorinated products with a factor of 2. The chemical oxygen demand (COD) was computed by determining the amount of oxygen required to oxidize the organic carbon and hydrogen in the external liquid phase compounds into water and carbon dioxide, respectively.

4.4 Comparison between model predictions and experimental results

The kappa number predictions correlated rather well with the experimental results (Figure 13). A systematic shortcoming appeared in predicting the very rapid initial kappa drop (during the first minute): the predicted kappa number at t = 1 min was consistently one unit higher than the experimental value. The extremely rapid initial HexA removal was well reproduced (Figure 14). The total magnitude of HexA removal was, however, underestimated. The HexA removal predictions fell short by 3-8 mmol/kg (Table 7, Figure 14). The predicted effect of the chemical dose on HexA removal was consistent with the experiments.

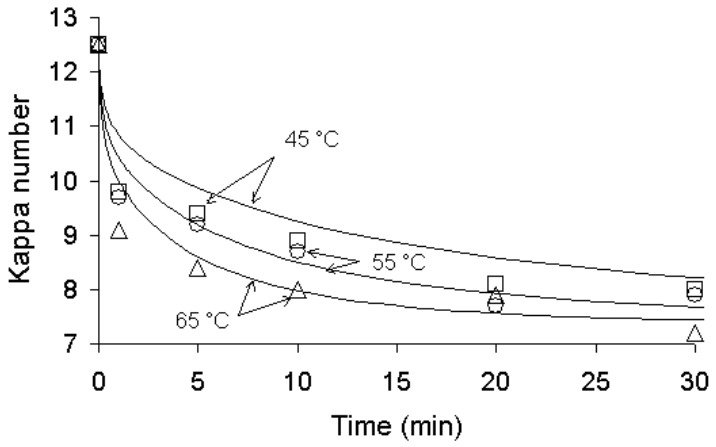

Figure 13. The predicted and experimental kappa number decrease at T = 45°C, 55°C and 65°C.

Table 7. Comparison of experimental and predicted pulp/liquor properties at a time of 30 min. Experimental results are taken from Lehtimaa et al (2010a, 2010b).

Pulp	Kappa		HexA (mmol/kg)		end pH		AOX (kg/ADt)		OX (kg/ADt)	
	Exp	Pred	Exp	Pred	Exp	Pred	Exp	Pred	Exp	Pred
O-delign pulp	12.5		45							
30 kg, 45°C	6.7	7.7	22	29	3.1	3.1	0.53	0.27	0.29	0.24
20 kg, 45°C	8.0	8.2	24	32	3.3	3.2	0.51	0.22	0.27	0.20
15 kg, 45°C	8.8	8.6	29	33	3.7	3.3	0.45	0.17	0.24	0.07
20 kg, 55°C	7.9	7.7	23	31	3.1	3.1	0.43	0.24	0.25	0.19
20 kg, 65°C	7.2	7.4	24	30	3.2	3.1	0.46	0.25	0.26	0.14

Table 8. Comparison of experimental and predicted oxychlorine concentrations at a time of 30 min. Experimental results are taken from Lehtimaa et al (2010a, 2010b).

Pulp	Chlorine dioxide (mmol/l)		Chlorite (mmol/l)		Chlorate (mmol/l)		Chloride (mmol/l)	
	Exp	Pred	Exp	Pred	Exp	Pred	Exp	Pred
30 kg, 45°C	2.4	4.5	0.3	1.9	2.2	0.5	8.0	8.7
20 kg, 45°C	0.5	1.5	0.3	1.9	1.7	0.4	7.2	7.7
15 kg, 45°C	0.2	0	1.2	3.6	0.9	0.2	4.5	5.6
20 kg, 55°C	0	1.0	0.2	1.3	1.6	0.6	6.5	8.5
20 kg, 65°C	0	0.5	0	1.4	1.4	0.7	7.5	8.9

The rapid initial phase of AOX generation was well predicted (Figure 15). However, the magnitude of the subsequent, relatively steady AOX generation (1-30 min) was severely underestimated. The trend (intensive initial phase) of OX formation was rather well estimated. The predicted effect of the chemical dose on organochlorine formation (OX and AOX) was much more dramatic than observed in the experiments. Splitting the chemical dose (30 kg → 15 kg) resulted in a 15% reduction in the final amount of AOX (t = 30 min) in the experiments. The predicted reduction was nearly 40% (Table 7). The effect on OX was overestimated as well (Figure 15). The temperature had a very small (AOX) or insignificant (OX) effect on experimental organochlorine formation. The predictions showed only a small temperature dependence on both AOX (directly proportional) and OX (inversely proportional) formation.

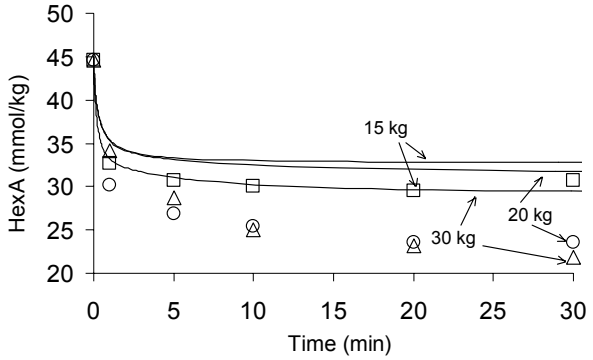

Figure 14. The predicted (line) and experimental (bullets) HexA content using with a dose of 30, 20, or 15 kg act. Cl/ADt chlorine dioxide.

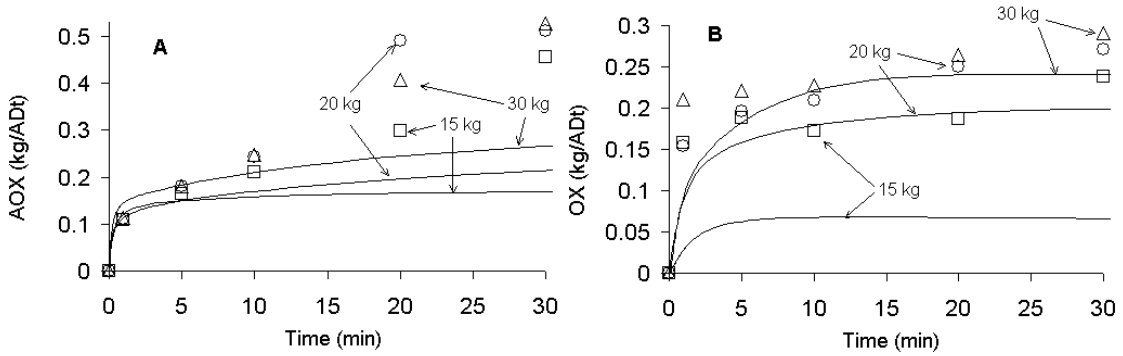

Figure 15. The predicted (line) and experimental (bullets) organochlorine formation with a dose of 30, 20, or 15 kg act. Cl/ADt chlorine dioxide.

The chlorine dioxide consumption predictions were coherent with the experimental results (Figure 16A). The amount of chlorite generated within the first minute was only slightly overestimated. The predicted chlorite depletion was slower than monitored in the experiments, especially for the low chemical dose (15 kg/ADt) experiment (Figure 16B). The trend in chlorate generation is correct, but the quantities fall severely short (Figure 16C). The simulated chloride ion concentration curves also have the right shape, but the total quantity is somewhat overestimated (Figure 16D).

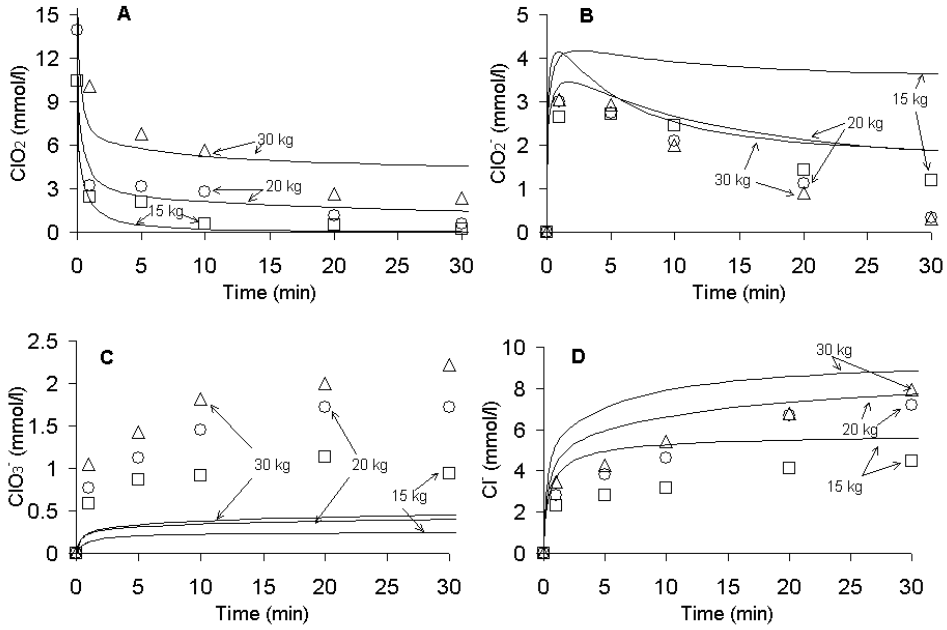

Figure 16. The predicted (line) and experimental (bullets) oxychlorine concentrations with a dose of 30, 20, or 15 kg act. Cl/ADt chlorine dioxide.

4.5 Discussion

4.5.1 Lignin reactions

The predictions offer several interesting topics of discussion regarding the applied theories and principles. The very rapid initial kappa drop could not be properly reproduced with the present models. This feature is likely to relate to lignin oxidation or dissolution, since the initial HexA removal was well predicted. One possibility is that the lignin reactions take place more extensively right on the surface of the fibers, so that dissolution into the external liquid is an immediate consequence of (fiber wall) lignin oxidation. Presently, the model operates so that the dissolving lignin fragments are first required to detach from the solid matrix and they then need to diffuse out of the fiber wall. The dissolved lignin compounds contribute to the kappa number during this process, as they remain inside the fiber wall liquid.

The ratio in which quinones, muconic acid esters, and the reactive intermediates are formed from the primary lignin offers another point of speculation. The first two structures are stable toward further oxidation and they consume a considerable amount of permanganate in the kappa number test (Table 6). Hence, if the fraction quinones and muconic acid esters being produced was overestimated, the initial kappa drop would be too small. Yet another explanation could arise from the division of lignin between phenolic (extremely reactive) and non-phenolic (very slow reaction) moieties. Although commonly used, the division may be too rough, and in reality some of the structures lumped into the non-phenolic category could be consumed at a substantial rate.

4.5.2 Chlorate formation

Chlorate formation was consistently underpredicted. Chlorous acid self-decomposition and iron-mediated chlorite depletion, both resulting in chlorate formation, have been found to have insignificant reaction rates above pH 3 [II, III]. The end pH was above 3 in each experiment and thus the only mechanism expected to produce chlorate would be the reaction between hypochlorous acid and chlorous acid. It appears that this route alone cannot account for the chlorate formation observed. This incoherence is unexpected, as the HOCl-$HClO_2$ reaction scheme and rate parameters were obtained under a very similar pH range and oxychlorine species composition as encountered in experiments [IV]. The presence of pulp, of course, makes a notable difference. Pulp suspensions present a heterogeneous environment, where the highly unstable Cl_2O_2 species may come across diffusional restrictions. If, for instance, the chloride ion content inside the fiber-bound liquid is not uniform, the local reaction paths of Cl_2O_2 could vary. The pulp-related compounds and structures might also participate in the Cl_2O_2 reactions, thereby affecting the reaction stoichiometry. The

extensive involvement of radical chemistry, initiated by sources other than ferric/ferrous ions, might also alter the predicted outcome (Lindgren and Nilsson 1975; Kolar and Lindgren 1982).

4.5.3 Hypochlorous acid driven processes

The predictions regarding HexA removal, chlorite depletion/chlorate formation, and organochlorine formation were not in complete agreement with the experimental results. The extent of each process was underestimated, especially at reaction times of 5-30 min. The common feature for these processes is that they all involve and compete for the intermediately formed hypochlorous acid. Figure 17 gives a principle presentation of the reaction scheme around hypochlorous acid. The underestimated reaction paths are bolded in gray. As the magnitude of all the aforementioned processes was underestimated, one obvious way to try to improve the model performance was to allocate a higher rate for one or all of these reactions. However, this was unsuccessful. Firstly, the present AOX formation, chlorite depletion, and HexA removal predictions fitted rather well during the first minutes of the reaction (0-5 min) and the deviations occurred only later. If any of the reaction paths was given a higher reaction rate, coherence in the later part improved, but at the expense of inferior correlation in the early part. In addition, as the reaction paths all compete for hypochlorous acid, assigning a higher rate for one reaction path suppresses the others and leads to a poorer general correlation in them. The reaction between chlorite/chlorous acid and lignin/carbohydrate aldehydes - an additional source for HOCl - was introduced in an attempt to improve the predictions. The reaction was defined to consume chlorite/chlorous acid and to produce hypochlorous acid, while converting the aldehydes into carboxylic acids (Jiang et al. 2007; Lehtimaa et al. 2007). An excess of aldehydes was assumed to be available. Introducing the aldehyde reaction resulted in much-improved Cl(III) concentration predictions, although improvements in HexA removal, AOX formation, and chlorate formation were rather insignificant.

The relative importance of the hypochlorous acid driven processes appeared to be temperature-independent. The experimental results showed that changes in temperature (45-65°C) had no effect on the rate or extent of HexA removal, OX formation, or chlorate formation. AOX formation was very slightly affected. Hence, temperature changes had no effect on the ratio in which the HOCl was consumed between the competing reaction paths. One explanation for this observation is that the initial reaction steps of each process have equal activation energies. A more likely possibility is that the hypochlorous acid, when formed, reacts so rapidly that it is instantly consumed by the nearest substrate, i.e. the hypochlorous acid consumption is diffusion-restricted. In this case the relative importance of the HOCl-consuming processes would not be determined by reaction kinetics, but by the internal structure and distribution of the substrates in the fiber wall. The simulations do not provide direct evidence to confirm this hypothesis, but the fact that the hypochlorous acid

concentration in the fiber-bound liquid was consistently almost an order of magnitude higher than in the external liquid (diffusional restrictions *between* the liquid phases) gives the hypothesis additional support.

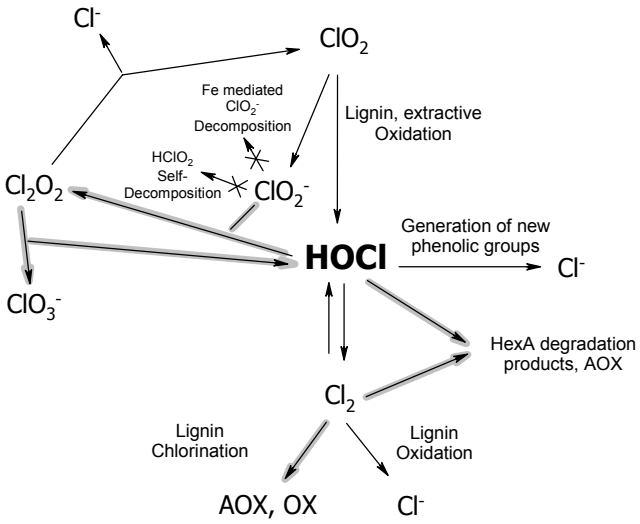

Figure 17. A simplified presentation of the oxychlorine reaction scheme operating in the model. Chlorous acid self-decomposition and iron-mediated chlorite decomposition are omitted, as their reaction rates are insignificant at pH above 3. Chlorination of phenols by HOCl is also omitted, since the reaction was found to be too slow to have an effect. The reaction paths whose importance was underestimated are bolded in gray.

It was surprising how little the experimental organochlorine formation was affected by the chemical dose (Table 7). The predicted dependence was much stronger. The model assumes chlorination by elemental chlorine to be unspecific with regard to lignin, i.e. all unoxidized lignin pseudo-compounds are chlorinated at equal rates. Thus, in the simulations, a higher chemical dose yields a higher amount of chlorine, which leads to more extensive chlorination. The fact that this scheme fails to predict the experimental outcome suggests that the chlorination process is not limited by the amount of chlorine, but by some other factor. One possibility is that chlorination is not unspecific, but occurs only via specific, chlorination-susceptible lignin structures and that the limiting factor is the abundance of these structures.

4.5.4 Chloride formation

The overestimation of chloride production is readily explained by the fact that too little chlorine ends up as chlorate and in organochlorine compounds. The chlorine balance must close, and the residual chlorine ends up as chloride and partly as chlorite.

5 SYNTHESIS OF THE PUBLICATIONS

This doctoral thesis consists of five papers. The overall objective was to first construct a phenomenon-based modeling environment for chemical pulp bleaching processes in general and then to focus in more detail on modeling chlorine dioxide bleaching. In the first part the main efforts were put in defining the required physico-chemical models, in defining how the pulp suspension environment should be modeled and how the massive amount of different fiber wall components and reactions would be implemented without making the model too complicated. The result is introduced in paper [I]. The examples given demonstrate that both electrolytes and neutral components may exhibit different concentrations inside the fiber wall and in the external liquid. Thus, it is essential to distinguish the two liquid phases and to acknowledge mass transfer restrictions between them. The existence of concentration gradient is not that common for neutral species, but evermore important as in these cases the effect is typically affiliated with highly reactive species. The practical significance of this topic lies in the fact that in experimental systems all samples and measurements are taken from the liquid external to fibers. Differences between the measured concentrations and those at the actual reactive sites inside the fibers may easily lead to false conclusions.

The second interest was in gathering a kinetic library for the reactions taking place during chlorine dioxide bleaching. In the bleaching process chlorine dioxide oxidizes various organic substrates, meanwhile going through a stepwise reduction to chloride. The reactions of the intermediate chlorine species are of utmost importance with respect to the overall red-ox efficiency of the bleaching process. The existing literature regarding the chemistry of these oxychlorine species was found inconsistent and new experiments were needed. Papers [II] and [IV] deal with the self-decomposition of chlorous acid and the reaction between the hypochlorous acid and chlorous acid, respectively. In both cases the reaction's temperature dependency was provided for the first time. Furthermore, this was the first time that chlorous acid self-decomposition results were reported at elevated temperatures and the reaction between hypochlorous acid and chlorous acid was studied at mildly acidic pH. Paper [III] reports a computational study of chlorate formation during chlorine dioxide delignification. Conclusions as to the conditions suppressing chlorate formation, i.e. to improving the red-ox efficiency of the bleaching process, were provided.

As a final part, paper [V] presents a phenomenon-based model for chlorine dioxide delignification. The results of the first two parts were exploited here. Descriptions as to how the reactions of residual lignin and other fiber wall components are modeled, how lignin dissolution is incorporated, and how the molecular scale composition in the fiber wall and in the liquor are converted into various measurable bulk variables (kappa number, COD, AOX, etc.) were provided. The model was validated

against experimental delignification results reported in detail by Lehtimaa et al (2010a, 2010b). The model combines a number of individual theories in predicting the outcome of the delignification process. The model is the first of its kind to be reported in pulp bleaching research. Its application opportunities in examining the cross-effects of individual theories and in identifying shortcomings in them were demonstrated. Several key variables including kappa number, chemical consumption, and pH were well predicted, yet discrepancies were encountered as well.

The pulp suspension model was also exploited in assessing the feasibility of $[AlMn(H_2O)W_{11}O_{39}]$ catalyzed oxygen (O_2) delignification (Ruuttunen et al. 2006). The central idea in this bleaching concept was to use $[AlMn(H_2O)W_{11}O_{39}]$ anion in mediating oxidizing power from molecular oxygen to lignin. The bleaching system was examined computationally after determining a number of unknown reaction kinetic parameters in the system. In the light of the simulation results, it was concluded that the suitability of the $[AlMn(H_2O)W_{11}O_{39}]$ anion as catalyst is questionable.

6 CONCLUSIONS AND SUGGESTIONS FOR FUTURE WORK

The results from the aqueous oxychlorine species studies were promising. The benefits of dividing complex reaction systems into smaller parts were clear. It was possible to reduce the amount of uncertainties and identify the rate parameters with improved confidence. Although the oxychlorine models performed well in fully aqueous systems, predictions regarding chlorite depletion and chlorate formation during pulp bleaching were deficient. It is difficult to judge whether the deviations resulted from omitting some pulp-related reactions, or from applying too many simplifications in modeling the fiber wall or pulp suspension structure. The challenge of simplifications was encountered also in the study dealing with of chlorate formation during chlorine dioxide delignification [III]. In lack of explicit information, several reaction kinetic or stoichiometric parameters had to be estimated, thus affecting adversely on the confidence of the predictions.

The phenomenon-based model presented for chlorine dioxide delignification is the first of its kind to be reported in the field of pulp bleaching research. The model combines several individual phenomenon models with a broad reaction kinetic library. This approach offers an exceptional opportunity to examine the validity of various theories or hypotheses and provide deeper knowledge regarding the bleaching process. In this work, for instance, the fact that both chlorate and organochlorine formation were underestimated suggests that our present conceptions regarding the reactions of intermediately formed hypochlorous acid are not insufficient. Also, the theory of unspecific chlorination by elemental chlorine was shown to be too simple to explain the experimentally observed chemical dose dependency in organochlorine formation. Despite these discrepancies, the the model gave good predictions for several key variables. Overall, the model was considered to meet the key expectations imposed.

The chlorine dioxide reaction library constructed in this work was used to model the delignification process, but it could as well be applied to simulate the brightening ClO_2 processes (D1 and D2 stages). The delignification and brightening processes involve the same phenomena and any condition related changes in the importance of the various reactions are incorporated implicitly. The model should, however, be extended to cover prediction of pulp brightness, as the overall objective of pulp bleaching is in color removal. In practice, adding this feature would require identification of the essential colored structures (chromophores) in pulp, creating reaction schemes for these structures, and linking the fiber wall chromophore content with pulp brightness. This task was left for future work.

The greatest challenges in constructing the model were encountered in validating the changes in fiber and liquor composition. The predominant ways to monitor changes in lignin composition/content and chlorinated organic compounds are structure unspecific (kappa number, COD, AOX, OX). Converting the molecular scale composition into these bulk variables brings an additional factor of complexity and uncertainty. The balance between model complexity and availability of proper validation data must be borne in mind when considering the future development of the model. The presently used set of unoxidized lignin pseudo-compounds is quite narrow (phenolic and non-phenolic moieties) and it would be interesting to introduce lignin categories such as β–O–4-, biphenyl-, and β-5-structures to improve the model credibility. These structures could be assigned specific reactivities and reaction paths. It would also be desirable to eliminate the rough assumption of uniform distribution and equal/full accessibility of lignin in the fiber wall. Several cell wall layers could be introduced and lignin could be assigned a heterogeneous distribution amongst them. Implementing such modifications, however, would require that suitable experimental results be available to define the cell wall layers and lignin categories, as well as tracking changes within them. Development of detailed, structure-specific analytical methods for characterizing the fiber wall and liquor would take the value of the model onto a whole new level.

While the in-depth development of chemistry and fiber wall models may be uncertain, there are several directions where the development prospects are bright. The present modeling concepts could be extended to cover other bleaching chemicals and unit operations. The chlorine dioxide reaction library may be replaced with reactions related to oxygen, hydrogen peroxide, ozone, or any other chemical to simulate other bleaching stages. The catalytic polyoxometalate bleaching study demonstrated that the modeling framework can be used also to examine ideas of new bleaching concepts, and that incorporating gaseous species (oxygen) or highly-charged anion clusters in the model does not cause problems. The phenomenon-based modeling concepts may also be extended to predict changes in fiber wall and liquor composition in pulp washing. The structure and characteristics of pulp as well as the essential phenomena remain the same; additional work would be required to model the filtrate flow arrangements.

NOTATION

a	activity of a component
c_i	component concentration (mol/kg fiber)
D	diffusion coefficient (m^2/s)
E_a	activation energy ($kJ \cdot mol^{-1}$)
H	hexenuronic acid content (mmol/kg)
K	equilibrium constant (reaction dependent)
k	rate constant (reaction dependent)
L	lignin content (weight %)
M_w	molar weight (g/mol)
N	mass transfer flux ($mol/(m^2 \cdot s)$)
R	gas constant ($8.3144\ J \cdot K^{-1} \cdot mol^{-1}$)
T	temperature (K)
t	time (min)
V	volume (m^3)
x	diffusion length (m);
z	ionic charge (-)

Greek symbols

ε	void fraction (-)
Δ	difference operator
κ	kappa number (-)
μ	viscosity (-)
τ	tortuosity coefficient (-)

Subscripts

eff	effective
i	component i

Abbreviations

act. Cl	active chlorine
AOX	adsorbable organic halogens
Cl(III)	sum of chlorite and chlorous acid
COD	chemical oxygen demand
DMSO	dimethylsulphoxide
EDTA	ethylenediamine-N,N,N',N'-tetraacetic acid

FSP	fiber saturation point
HexA	hexenuronic Acid
HMW	high molecular weight
MA	maleic acid
NPL	non-phenolic lignin
OA	oxalic acid
o.d.	oven dry
OX	organically-bound chlorine in fibers
OxEq	oxidation equivalent
pK_a	10-base logarithm of dissociation coefficient K_a
POM	polyoxometalate

LITERATURE CITED

Aieta, E.M., and Roberts, P.V., Application of mass-transfer theory to the kinetics of a fast gas-liquid reaction: chlorine hydrolysis, *Environ. Sci. Technol.* **20** (1986a) 44-50.

Aieta, E.M., and Roberts, P.V., Kinetics of the reaction between molecular chlorine and chlorite in aqueous solution, *Environ. Sci. Technol.* **20** (1986b) 50-55.

Ala-Kaila,K., Modeling of mass transfer phenomena in pulp-water suspensions, (1998), Ph.D. Thesis, Helsinki University of Technology, Espoo, Finland.

Alén, R., Structure and chemical composition of wood, in *Papermaking Science and Technology, Book 3: Forest Products Chemistry*, Stenius, P. (ed.), (2000), Fapet Oy, Helsinki, Finland, 40.

Anon., *Trends in World Bleached Chemical Pulp Production: 1990-2005*. Alliance for Environmental Technology. May 2006.

Barroca, M.J.M.C., Simoes, R.M.S., Almiro, J., and Castro, A.M., Kinetics of chlorine dioxide delignification of a hardwood kraft pulp, *Appita J.* **54** (2001) 190-195.

Bergnor, E., Germgard, U., Kolar, J.J., and Lindgren, B.O., Formation of chlorate in chlorine dioxide bleaching, *Cell. Chem. Technol.* **21** (1987) 307-314.

Björklund, M., Germgård, U., Basta, J., Formation of AOX and OCl in ECF bleaching of birch pulp, *Tappi J.* 2004, **3**(8), 7-11.

Brage, C., Eriksson, T., and Gierer, J., Reactions of chlorine dioxide with lignins in unbleached pulps. Part I. Reactions of chlorine dioxide with monomeric model compounds representing aromatic structures in residual lignins, *Holzforschung* **45** (1991a) 23-30.

Brage, C., Eriksson, T., and Gierer, J., Reactions of chlorine dioxide with lignins in unbleached pulps. Part II. Reactions of chlorine dioxide with dimeric model compounds representing aromatic structures in residual lignins, *Holzforschung* **45** (1991b) 147-151.

Brogdon, B.N., Influence of oxidized lignin structures from chlorine dioxide delignified pulps on the kappa number test, *J. Pulp Paper Sci.* **27** (2001) 364-369.

Bygrave, G., and Englezos, P., Thermodynamics-based model and data for Ca, Mg, and Na ion partitioning in kraft pulp fibre suspensions, *Nord. Pulp Paper Res. J.* **15** (2000) 155-159.

Chandranupap, P., and Nguyen, K.L., Effect of pH on kinetics and bleaching efficiency of chlorine dioxide delignification, *Appita J.* **53** (2000) 4-4 pp.

Connick, R.E., and Chia, Y., The hydrolysis of chlorine and its variation with temperature, *J. Am. Chem. Soc.* **81** (1959) 1280-1284.

Costa, M.M., and Colodette, J.L., The impact of kappa number composition on eucalyptus kraft pulp bleachability, *Brazil. J. Chem. Eng.* **24** (2007) 61-71.

Cussler, E.L., *Diffusion, mass transfer in fluid systems,* (1984), Cambridge University Press, Cambridge, U.K.

Dahlman, O., Reimann, A., Stromberg, L., Morck, R., High-molecular-weight effluent materials from modern ECF and TCF bleaching, *Tappi J.* 1995, **78** (12), 99-109.

Dahlman, O., Reimann, A., Ljungquist, P., Morck, R., Johansson, C., Boren, H., and Grimvall, A., Characterization of chlorinated aromatic structures in high-molecular-weight BKME materials and in fulvic acids from industrially unpolluted waters, *Water Sci.Technol.* **29** (1994) 81-91.

Dean, J.A., *Lange's Handbook of Chemistry*, (1999), McGraw-Hill Inc., New York, USA,

Deborde, M., and von Gunten, U., Reactions of chlorine with inorganic and organic compounds during water treatment - Kinetics and mechanisms: A critical review, *Water Res.* **42** (2008) 13-51.

Dence, C.W., Gupta, M.K., and Sarkanen, K.V., Studies on oxidative delignification mechanisms. II. Reactions of vanillyl alcohol with chlorine dioxide and sodium chlorite, *Tappi* **45** (1962) 29-38.

Dence, C.W., and Reeve, D.W., *Pulp Bleaching: Principles and Practice,* (1996), Tappi Press, Atlanta, GA, United States.

Eigen, M., and Kustin, K., Kinetics of halogen hydrolysis, *J. Am. Chem. Soc.* **84** (1962) 1355-1361.

Emmenegger, F., and Gordon, G., The rapid interaction between sodium chlorite and dissolved chlorine, *Inorg. Chem.* **6** (1967) 633-635.

Fabian, I., The reactions of transition metal ions with chlorine(III), *Coord. Chem. Rev.* **216-217** (2001) 449-472.

Fabian, I., and Gordon, G., Iron(III)-catalyzed decomposition of the chlorite ion: an inorganic application of the quenched stopped-flow method, *Inorg. Chem.* **31** (1992) 2144-2150.

Fabian, I., and Gordon, G., Kinetics and mechanism of the complex formation of the chlorite ion and iron(III) in aqueous solution, *Inorg. Chem.* **30** (1991) 3994-3999.

Fogelholm, C.J., *Papermaking science and technology 6A. Chemical pulping,* (2000), Fapet Oy, Jyväskylä.

Fredricks, P.S., Lindgren, B.O., and Theander, O., Chlorine oxidation of cellulose IV. Kinetics and mechanisms of the reactions of methyl b-D-glucopyranoside with chlorine in acid aqueous solution, *Svensk Papperstidning* **74** (1971) 597-603.

Freire, C.S.R., Silvestre, A.J.D., and Pascoal Neto, C., Oxidized derivatives of lipophilic extractives formed during hardwood kraft pulp bleaching, *Holzforschung* **57** (2003) 503-512.

Froment, G.F., and Bischoff, K.B., *Chemical reactor analysis and design,* (1990), John Wiley & Sons, New York, USA.

Germgård, U., Kinetics of prebleaching softwood kraft pulp with chlorine dioxide and small fractions of chlorine, *Pap.Puu* **64** (1982) 76-82.

Germgård, U., Teder, A., and Tormund, D., Chlorate formation during chlorine dioxide bleaching of softwood kraft pulp, *Pap. Puu* **63** (1981) 127-133.

Gordon, G., and Tachiyashiki, S., Kinetics and mechanism of formation of chlorate ion from the hypochlorous acid/chlorite ion reaction at pH 6-10. *Environ. Sci. Technol.* **25** (1991) 468-474.

Gordon, G., Kieffer, R.G., and Rosenblatt, D.H., The chemistry of chlorine dioxide, *Prog. Inorg. Chem.* **15** (1972) 201-286.

Gunnarsson, N.P.-I., and Ljunggren, S.C.H., Kinetics of lignin reactions during chlorine dioxide bleaching, 1: Influence of pH and temperature on the reaction of 1-(3,4-Dimethoxyphenyl) ethanol with chlorine dioxide in aqueous solution, *Acta Chem. Scand.* **50** (1996) 422-431.

Hamzeh, Y., Evaluation de nouveaux procedes de delignification et blanchement en reacteur a deplacement de liqueur, et comparison avec les procedes traditionnels, (2005), Ph.D Thesis, EFPG, Grenoble, France.

Helfferich, F., *Ion exchange,* (1962), McGraw-Hill, New York.

Hoigne, J., and Bader, H., Kinetics of reactions of chlorine dioxide (OClO) in water - I. Rate constants for inorganic and organic compounds, *Water Res.* **28** (1994) 45-55.

Hong, C.C., and Rapson, W.H., Kinetics of disproportionation of chlorous acid, *Can. J. Chem.* **46** (1968) 2053-2060.

Horvath, A.K., Nagypal, I., Peintler, G., Epstein, I.R., and Kustin, K., Kinetics and mechanism of the decomposition of chlorous acid. *J. Phys. Chem. A* **107** (2003) 6966-6973.

Jakobsson, K., and Aittamaa, J., *KINFIT User's Manual,* http://www.tkk.fi/Units/ChemEng/research/Software/kinfit/KINFIT_eng.html.

Jansson, M.B., Wormald, P., and Dahlman, O., Reactions of wood extractives during ECF and TCF bleaching of kraft pulp, *Pulp Pap. Canada* **96** (1995) 42-45.

Jia, Z., Margerum, D.W., and Francisco, J.S., General-acid-catalyzed reactions of hypochlorous acid and acetyl hypochlorite with chlorite, *Ion. Inorg. Chem.* **39** (2000) 2614-2620.

Jiang, Z., Van Lierop, B., and Berry, R., Improving chlorine dioxide bleaching with aldehydes, *J. Pulp Paper Sci.* **33** (2007) 89-94.

Joncourt, M.J., Froment, P., Lachenal, D., and Chirat, C., Reduction of AOX formation during chlorine dioxide bleaching, *Tappi J.* **83** (2000) 144-148.

Juutilainen, S., Vuorinen, T., Vilpponen, A., Henricson, K., and Pikka, O., Combining chlorine dioxide bleaching of birch kraft pulp with an a-stage at high temperatures, *TAPPI pulping conference*, (1999), Orlando, FL, USA, vol. 2, pp 645-651.

Kieffer, R.G., Stoichiometry and kinetics of the disproportionation of chlorous acid, (1967) 120 pp.

Kieffer, R.G., and Gordon, G., Disproportionation of chlorous acid. II. Kinetics. *Inorg. Chem.* **7** (1968a) 239-244.

Kieffer, R.G., and Gordon, G., Disproportionation of chlorous acid. I. Stoichiometry. *Inorg. Chem.* **7** (1968b) 235-239.

Kolar, J.J., and Lindgren, B.O., Oxidation of styrene by chlorine dioxide and by chlorite in aqueous solutions, *Acta Chem. Scand.* ***36 B*** (1982) 599-605.

Kolar, J.J., Lindgren, B.O., and Pettersson, B., Chemical reactions in chlorine dioxide stages of pulp bleaching: Intermediately formed hypochlorous acid, *Wood Sci. Technol.* **17** (1983) 117-128.

Lachenal, D., Chirat, C., Improvement of ClO_2 delignification in ECF bleaching, *Proceedings of IPBC 2000*, (2000), Halifax, NS, Canada, 185-188.

Laine, J., Lövgren, L., Stenius, P., and Sjöberg, S., Potentiometric titration of unbleached kraft cellulose fiber surfaces, *Colloids Surf. A* **88** (1994) 277-287.

Laliberte, M., Model for calculating the viscosity of aqueous solutions, *J. Chem. Eng. Data* **52** (2007a) 321-335.

Laliberte, M., Model for calculating the viscosity of aqueous solutions, *J. Chem. Eng. Data* **52** (2007b) 1507-1508.

Lehtimaa, T,. Tarvo, V., Kuitunen, S., Jääskeläinen, A.-S., Vuorinen, T., The effect of process variables in chlorine dioxide prebleaching of birch kraft pulp. Part 1. Inorganic chlorine compounds, kappa number, lignin and hexenuronic acid content, *J. Wood Chem. Technol.* **30** (2010a) 1-18.

Lehtimaa, T,. Tarvo, V., Kuitunen, S., Jääskeläinen, A.-S., Vuorinen, T., The effect of process variables in chlorine dioxide prebleaching of birch kraft pulp. Part 2. AOX and OX formation, *J. Wood Chem. Technol.* **30** (2010b) 19-30.

Lehtimaa, T., Tarvo, V., Mortha, G., and Vuorinen, T., The role of chlorite in chlorine dioxide bleaching, *Proc. 14th ISWFPC*, (2007), Durban, South Africa.

Li, J., Sevastyanova, O., and Gellerstedt, G., The relationship between kappa number and oxidizable structures in bleached kraft pulps, *J. Pulp Paper Sci.* **28** (2002) 262-266.

Li, J., and Gellerstedt, G., On the structural significance of the kappa number measurement, *Nord. Pulp Paper Res. J.* **13** (1998) 153-158.

Li, J. and Gellerstedt, G. The contribution to kappa number from hexeneuronic acid groups in pulp xylan, *Carbohydr. Res.* **302** (1997) (3-4), 213-218.

Lindgren, B.O., Chlorine dioxide and chlorite oxidations of phenols related to lignin, *Svensk papperstidn.* **74** (1971) 57-63.

Lindgren, B.O., and Nilsson, T., Chlorate formation during reaction of chlorine dioxide with lignin model compounds, *Svensk papperstidn.* **78** (1975) 66-68.

Lindgren, J., Wiklund, L., and Öhman, L., The contemporary distribution of cations between bleached softwood fibres and the suspension liquid, as a function of -log[H^+], ionic strength and temperature, *Nord. Pulp Paper Res. J.* **16** (2001) 24-32.

Marpillero, P., The bleaching of pulps with activated chlorate, *Tappi* **41** (1958) 213A-216A.

McKague, A.B., Reeve, D.W., and Xi, F., Reaction of lignin model compounds sequentially with chlorine dioxide and sodium hydroxide, *Nord.Pulp Paper Res. J.* **10** (1995) 114-118.

McKague, A.B., Kang, G.J., and Reeve, D.W., Reactions of lignin model dimers with chlorine dioxide, *Nord.Pulp Pap.Res.J.* **9** (1994) 84-87, 128.

Medina, J., Lehtimaa, T., Tervola, P., Vehmaa, J., Pikka, O., and Vuorinen, T., Chlorate reduction in Eucalyptus pulp bleaching, *IPBC Conference Proc*, (2008), Quebec City, Canada, PAPTAC.

Mortha, G., Lachenal, D., and Chirat, C., Modeling multistage chlorine dioxide bleaching, *Proc.11th ISWPC*, (2001), Nice, France, Association Technique de l'Industrie Papetière, 447-451.

Newman, J.S., *Electrochemical systems,* (1991), Prentice-Hall, New Jersey.

Ni, Y., Kubes, G.J., and Van Heiningen, A.R.P., Development of phenolic lignin during chlorine dioxide bleaching of kraft pulp, *J. Wood Chem. Technol.* **15** (1995)

Ni, Y., Shen, X.H., and van Heiningen, A.R.P., Studies on the reactions of phenolic and nonphenolic lignin model compounds with chlorine dioxide, *J. Wood Chem. Technol.* **14** (1994) 243-262.

Ni, Y., Kubes, G.J., and Van Heiningen, A.R.P., Mechanism of chlorate formation during bleaching of kraft pulp with chlorine dioxide, *J. Pulp Paper Sci.* **19** (1993) J1-J6.

Ni, Y., Kubes, G.J., and Van Heiningen, A.R.P., New mechanism for pulp delignification during chlorination, *J. Pulp Paper Sci.* **16** (1990) 13-19.

Nicoson, J.S., and Margerum, D.W., Kinetics and mechanisms of aqueous chlorine reactions with chlorite ion in the presence of chloride ion and acetic acid/acetate buffer, *Inorg. Chem.* **41** (2002) 342-347.

Nilsson, T., and Sjöström, L., Losses in chlorine dioxide as a result of chlorate formation during bleaching, *Svensk papperstidn.* **77** (1974) 643-7.

Norgren, M., and Lindström, B., Dissociation of phenolic groups in kraft lignin at elevated temperatures, *Holzforschung* **54** (2000a) 519-527.

Norgren, M., and Lindström, B., Physico-chemical characterization of a fractionated kraft lignin, *Holzforschung* **54** (2000b) 528-534.

Ondrus, M.G., and Gordon, G., Oxidation of hexaaquoiron(II) by chlorine(III) in aqueous solution, *Inorg. Chem.* **11** (1972) 985-989.

Peintler, G., Nagypal, I., and Epstein, I.R., Systematic design of chemical oscillators. 60. Kinetics and mechanism of the reaction between chlorite ion and hypochlorous acid, *J. Phys. Chem.* **94** (1990) 2954-2958.

Perry, R.H., and Green, D.W., *Perry's Chemical Engineers' Handbook*, (1997), McGraw-Hill, UK.

Ragnar, M., Lindgren, C.T., and Nilvebrant, N., pK_a-values of guaiacyl and syringyl phenols related to lignin, *J. Wood Chem. Technol.* **20** (2000) 277-305.

Rapson, W.H., and Anderson, C.B., Kraft pulp bleaching with chlorine and chlorine dioxide - effect of pH on the chlorination stage, *Tappi J.* **61** (1978) 97-99.

Rapson, W.H., and Anderson, C.B., Improving the efficiency of chlorine dioxide bleaching, *Transactions Tech. Sect. CPPA* **3** (1977) TR52-TR55.

Räsänen, E., Stenius, P., and Tervola, P., Model describing Donnan equilibrium, pH and complexation equilibria in fibre suspensions, *Nord. Pulp Paper Res. J.* **16** (2001) 130-139.

Räsänen,E., Modelling ion exchange and flow in pulp suspension, (2003), Ph.D. Thesis, VTT Processes, Espoo, Finland.

Rebenne, L.M., Gonzalez, A.C., and Olson, T.M., Aqueous chlorination kinetics and mechanism of substituted dihydroxybenzenes, *Environ. Sci. Technol.* **30** (1996) 2235-2242.

Reid, R.C., Prausnitz, J.M., and Poling, B.E., *The properties of gases and liquids,* (1987), McGraw-Hill, New York, USA.

Ruuttunen, K., Tarvo, V., Aittamaa, J., Vuorinen, T., $[AlMn^{II}(H_2O)W_{11}O_{39}]^{7-}$ Anion oxidation kinetics and simulative overall studies of catalytic oxygen bleaching, *Nord. Pulp Paper Res. J.* **21** (2006) 303-313.

Savoie, M., and Tessier, P., Mathematical model for chlorine dioxide delignification, *Tappi J.* **80** (1997) 105, 112, 119, 145-153.

Schmitz, G., and Rooze, H., Reaction mechanism for chlorite and chlorine dioxide. 3. Disproportionation of chlorite, *Can. J. Chem.* **63** (1985) 975-980.

Schmitz, G., and Rooze, H., Reaction mechanism for chlorite and chlorate. 2. Reaction kinetics of chlorite in the presence of o-tolidine, *Can. J. Chem.* **62** (1984) 2231-2234.

Schmitz, G., and Rooze, H., Reaction mechanisms for chlorite and chlorine dioxide. 1. Stoichiometry of chlorite reactions and kinetics in the presence of ortho-toluidine, *Can. J. Chem.* **59** (1981) 1177-1187.

Sixta, H., Suess H-Y, Potthast, A., Schwanninger, M., and Krotscheck, A., Pulp bleaching, in: *Handbook of Pulp, Vol 2,* Sixta, H. (ed.), (2006), Wiley-VCH Verlag GmbH, Weinheim, 609.

Soila, R., Lehtikoski, O., and Virkola, N.-E., On the reactions taking place during the chlorine dioxide bleaching stage, *Svensk papperstidn.* **65** (1962) 632-638.

Soper, F.G., and Smith, G.F., Halogenation of phenols, *J. Chem. Soc.* (1926) 1582-1591.

Svenson, D.R., Kadla, J.F., Chang, H., and Jameel, H., Effect of pH on the inorganic species involved in a chlorine dioxide reaction system, *Ind. Eng. Chem. Res.* **41** (2002) 5927-5933.

Svenson, D.R., Jameel, H., Chang, H., and Kadla, J.F., Inorganic reactions in chlorine dioxide bleaching of softwood kraft pulp, *J. Wood Chem. Technol.* **26** (2006) 201-213.

Taube, H., and Dodgen, H., Applications of radioactive chlorine to the study of the mechanisms of reactions involving changes in the oxidation state of chlorine, *J. Am. Chem. Soc.* **71** (1949) 3330-3336.

Teleman, A., Harjunpää, V., Tenkanen, M., Buchert, J., Hausalo, T., Drakenberg, T., and Vuorinen, T., Characterisation of 4-deoxy-*beta*-L-*threo*-hex-4-enopyranosyluronic acid attached to xylan in pine kraft pulp and pulping liquor by ^{1}H and ^{13}C NMR spectroscopy, *Carbohydr. Res.* **272** (1995) 55-71.

Tessier, P., and Savoie, M., Chlorine dioxide delignification kinetics and EOP extraction of softwood kraft pulp, *Can. J. Chem. Eng.* **75** (1997) 23-30.

Towers, M., and Scallan, A.M., Predicting the ion-exchange of kraft pulps using Donnan theory, *J. Pulp Paper Sci.* **22** (1996) J332-J337.

Van Wijk, D.J., and Hutchinson, T.H., The ecotoxicity of chlorate to aquatic organisms: A critical review, *Ecotox. Environ. Safe.* **32** (1995) 244-253.

Vilen, E. J.; McKague, A. B.; Reeve, D. W. Quantification of muconic acid-type structures in high molecular weight material from bleach plant effluents, *Holzforschung* **54** (2000) 273-278.

Voudrias, E.A., and Reinhard, M., Reactivities of hypochlorous and hypobromous acid, chlorine monoxide, hypobromous acidium ion, chlorine, bromine, and bromine chloride in electrophilic aromatic substitution reactions with *p*-xylene in water, *Environ. Sci. Technol.* **22** (1988) 1049-1056.

Vuorinen, T., Fagerstrom, P., Räsänen, E., Vikkula, A., Henricson, K., and Teleman, A., Selective hydrolysis of hexenuronic acid groups opens new possibilities for development of bleaching processes, *9th ISWPC*, (1997), Montreal, Que, Canada, M4-1-M4-4.

Wajon, J.E., Rosenblatt, D.H., and Burrows, E.P., Oxidation of phenol and hydroquinone by chlorine dioxide, *Environ. Sci. Technol.* **16** (1982) 396-402.

Wang, T.X., and Margerum, D.W., Kinetics of reversible chlorine hydrolysis: temperature dependence and general-acid/base-assisted mechanisms, *Inorg. Chem.* **33** (1994) 1050-1055.

Wartiovaara, I., The influence of pH on the D1 stage of a D/CED1 bleaching sequence, *Pap. Puu* **64** (1982) 534, 539-40, 545.

Yoon, B., Wang, L., Yoon, S., and Kim, S., Mechanism of chlorate formation in chlorine dioxide delignification, *Appita J.* **57** (2004) 472-474.

Zhang, X.Z., Ni, Y., and Van Heiningen, A.R.P., Effect of consistency on chemical pulp ozonation; calculation of the effective capillary cross-sectional area (ECCSA) and tortuosity (l) of the fiber wall, *5th European Workshop on Lignocellulosics and Pulp*, (1998), Aveiro, Portugal, 413-416.

Österberg, F. and Lindström, K. Characterization of High-Molecular-Mass Chlorinated Matter in Spent Bleach Liquors (SBL). (2). Acidic SBL. *Holzforschung* **39** (1985) 149-158.